IEEE Access
Multidisciplinary | Rapid Review | Open Access Journal

Received 16 May 2024, accepted 6 June 2024, date of publication 10 June 2024, date of current version 18 June 2024.

Digital Object Identifier 10.1109/ACCESS.2024.3411929

RESEARCH ARTICLE

DeepRISBeam: Deep Learning-Based RIS Beam Management for Radio Channel Optimization

IACOVOS I. IOANNOU[1,2], (Member, IEEE), MARIOS RASPOPOULOS[3], (Member, IEEE), PRABAGARANE NAGARADJANE[4], CHRISTOPHOROS CHRISTOPHOROU[1,2], WAQAR ALI AZIZ[1,2], VASOS VASSILIOU[1,2], (Senior Member, IEEE), AND ANDREAS PITSILLIDES[1,5]

[1]Department of Computer Science, University of Cyprus, 1678 Nicosia, Cyprus
[2]Centre of Excellence (CYENS), 1678 Nicosia, Cyprus
[3]School of Sciences, University of Central Lancashire, 7080 Pyla, Cyprus
[4]Department of ECE, Sri Sivasubramaniya Nadar College of Engineering, Chennai 603110, India
[5]Department of Electrical and Electronic Engineering Science, University of Johannesburg, Johannesburg 2006, South Africa

Corresponding author: Iacovos I. Ioannou (ioannou.iakovos@ucy.ac.cy)

This was supported in part by the European Union's Horizon 2020 Research and Innovation Program under Grant 739578; in part by the ADROIT6G Project of the Smart Networks and Services Joint Undertaking (SNS-JU) under Grant 101095363; and in part by the Government of the Republic of Cyprus through the Deputy Ministry of Research, Innovation, and Digital Policy.

ABSTRACT In the rapidly developing field of wireless communication, the control of beams in Reconfigurable Intelligent Surfaces (RISs) has emerged as a promising element beyond 5G wireless communication systems. Due to their distinctive reflecting elements, Reconfigurable Intelligent Surface (RIS) is essential in several operations, including beamforming and beam steering. However, the optimization of these functions necessitates complex solutions. In this study, the authors introduce the Feedback DNN strategy, which combines the Feedback Neural Network and Deep Neural Network techniques specifically designed for channel estimation. This methodology utilizes deep neural networks to provide the RIS and user equipment communication path, enabling improved beamforming and steering capabilities. This study highlights the incorporation of machine learning (ML) within the field of communication engineering, intending to enhance the reliability and effectiveness of wireless communication systems. The contributions encompass a novel methodology for managing RIS beams, sophisticated approaches for channel estimates, optimization of beam operations, and the potential to enhance the performance of wireless systems by utilizing RISs via a Feedback DNN (called DeepRISBeam). The proposed approach is compared against other state-of-the-art ML approaches regarding their training accuracy. At the same time, it evaluated Bit Error Rate performance in high- and low-mobility vehicular communication scenarios.

INDEX TERMS RIS, feedback DNN, machine learning, wireless performance, energy efficiency, energy harvesting, green.

I. INTRODUCTION

The effective control of beams, particularly within the framework of Reconfigurable Intelligent Surfaces (RISs), plays a vital role in the evolution of modern wireless communication systems [1]. Beam management in RIS addresses the challenge of optimizing the propagation direction of wireless signals in communication systems. RISs, composed of numerous reflecting elements, can reconfigure these elements to modify the direction of signals that interact with them. Thus, RISs, sometimes called Intelligent Reflecting Surfaces (IRS), are characterized by their ability to alter the direction and phase of incoming signals through an array of programmatically configurable reflecting elements [2]. These capabilities are crucial for the execution of beamforming and beam steering operations, as they improve

The associate editor coordinating the review of this manuscript and approving it for publication was Li Minn Ang.

signal directionality and enhance communication reliability and efficiency in a controllable way. The main obstacle pertains to optimizing beam management to achieve optimal levels of throughput and reliability. An innovative approach utilizing Artificial Intelligence (AI) is suggested in response to this matter. The Feedback Recurrent Neural Network (RNN) is specifically designed for channel estimation. At the same time, by harnessing the capabilities of deep learning, it becomes feasible to precisely estimate the channel connecting the RIS and the user equipment (UE). Gaining insights into this channel enables fine-tuning of beamforming and beam steering, ensuring optimal communication even in challenging environments [3]. Moreover, the Feedback DNN architecture, renowned for processing sequences and feedback loops, is a deep-learning approach suitable for modeling and comprehending dynamic systems like wireless channels.

The precise assessment of channel characteristics is not solely a theoretical endeavor but plays a crucial role in effectively implementing RISs in real-world scenarios. An accurate estimation guarantees the ability to dynamically control radio beams to improve wireless propagation conditions and mitigate interference or signal degradation efficiently or even provide a means of wireless physical security. The main aim of this study is to address the difficulties associated with beam management in the context of RIS in contemporary wireless systems [4], [5], [6]. This study emphasizes the significance of utilizing AI to enhance beam management procedures and the system's overall performance. Most specifically, it focuses on effectively controlling the angle of reflection on the RIS to optimize the power received at the receiver and let the device harvest from this power by achieving a specific selected data rate. The introduction of the Feedback DNN technique represents a notable example of the seamless integration between deep learning and communication engineering, with a particular focus on channel estimation. RISs that have demonstrated their capability to enhance system performance by modulating signal propagation, hence revolutionizing wireless communication, offer a promising avenue for further advancements. The integration of AI with wireless communication technologies presents significant prospects concurrently. The significance of accurate channel estimates between the RIS and UE is highlighted by concrete, practical obstacles that potentially undermine the quality of the transmitted signal. However, these can be addressed by utilizing effective beam management, which is enhanced by the meticulous estimate of channel characteristics. Moreover, conventional techniques may be inadequate, considering beam management difficulties' especially the fact that channels might be complex and diverse. This study is focused on adopting an AI-focused methodology that can improve channel estimation and beam management results.

The primary innovation presented is introducing the Feedback DNN approach and other ML approaches (i.e., LSTM, BLSTM, RNN_BLSTM, RNN) specifically for channel estimation within the context of RIS. Rather than relying on traditional beam management techniques, the authors employ deep neural networks to estimate the channel between the RIS and UE. This novel integration of advanced neural network models into RIS beam management aims to optimize the pivotal aspects of beamforming and beam steering.

The specific contributions in this paper are:

1) *Integration of Neural Networks in RIS Beam Management*: Proposes a modern approach to the traditional problem of beam management in wireless communications by integrating Feedback DNN, a deep neural network, into RISs.
2) *Advanced ML-based Channel Estimation*: Proposes a method to estimate the RIS-UE channel utilizing ML. This detailed channel information is essential for optimizing beam-related operations.
3) *Optimization of Beamforming and Beam Steering for improved overall wireless performance*: Demonstrate the signal and overall performance improvement due to the better beam management approach resulting from the precise channel estimation.

The rest of the paper is structured as follows. Section II provides some background information on the RIS and the ML approaches used in this examination. It also offers related work on approaches addressing the energy and data rate optimization and energy of RIS using ML. The assumptions, terms, problem description, and formulation, including an overview of how the investigated approaches are associated with the optimization objective, are elaborated in Section III. The methodology used, the model training details, the dataset creation algorithm for the ML training and testing, and the algorithm that the BS should execute to predict the best-reflecting angles in the RIS are provided in Section IV. The efficiency of the investigated approaches is examined, evaluated, and compared in Section V in high and low mobility scenarios. Finally, Section VI includes concluding remarks and our future directions.

II. BACKGROUND KNOWLEDGE AND RELATED WORK

A. BACKGROUND KNOWLEDGE

1) RECONFIGURABLE INTELLIGENT SURFACES

RISs have garnered significant attention as a transformative technology to reshape wireless environments, boost energy efficiency, and enhance communication system performance. The two domains have naturally converged with the rise of ML in optimizing wireless communication systems. The conceptual melding of RIS and ML seeks to optimize RIS settings based on varying wireless conditions. Early works such as those by Renzo et al. [7] provided insights into smart radio environments, wherein RIS was a component of a broader system empowered by ML techniques. While the amalgamation of ML and RIS is still nascent, the potential appears to be vast. Future directions may include more complex ML models tailored to specific RIS architectures or exploring unsupervised and semi-supervised learning

techniques for further system optimization. In summary, the convergence of ML and RIS is poised to bring forth innovative solutions and improvements in wireless communication, paving the way for more intelligent and adaptive wireless environments.

RIS are emerging technologies in wireless communication that manipulate electromagnetic waves to improve signal quality and network performance. They are surfaces with numerous tiny electronic elements that can dynamically adjust their properties to control the reflected signals' phase, amplitude, or polarization. There are two types of RIS:

- **Passive RIS:** Refers to surfaces that can alter the properties of incident electromagnetic waves without the need for external power sources to amplify the signal. These surfaces rely on passive components, such as varactors or PIN diodes, to modulate the signal. The main limitation of passive RIS is the ''double path fading effect,'' where the signal power decays with the square of the distance both on the link from the transmitter to the RIS and from the RIS to the receiver, leading to a significant reduction in the received signal strength.
- **Active RIS:** Includes active components such as amplifiers within the surface, which can boost the signal power. This capability addresses the double path fading effect by amplifying the reflected signal, thereby enhancing the overall system performance, especially in terms of signal strength and coverage area. Active RIS can actively control the signal, offering the potential for better optimization of wireless networks by compensating for signal loss more effectively than their passive counterparts.

The transition from passive to active RIS opens up new opportunities for addressing the inherent limitations of passive systems, particularly in scenarios where maintaining signal strength over longer distances is crucial.

When comparing passive and active RIS within the same power budget, the superiority of one over the other largely depends on specific application requirements and constraints. Active RIS, with its integrated amplifiers, boosts the signal power, thus directly addressing the double path fading effect and potentially offering superior signal strength and coverage performance. This capability makes active RIS particularly appealing for scenarios requiring long-distance communication or where signal attenuation is a significant issue. The active control over the signal also allows for more dynamic and effective wireless network optimization. However, including amplifiers in active RIS increases the system's power consumption. When operating within a strict power budget, the additional power used for signal amplification must be considered against the total power available. Therefore, the efficiency of active RIS depends on its ability to significantly enhance signal quality or coverage without exceeding the allocated power budget. Overall, the active RIS can be used when the energy consumption at an RIS is not an issue. However, in most cases, there are battery power limitations in the RIS matrices; thus, in these cases, the passive RIS should be selected.

In discussing the superiority of active versus passive RIS in a paper, it is crucial to analyze the trade-offs between the enhanced performance offered by active components and the additional power consumption they entail. This discussion should also consider the specific use case scenarios where the benefits of active RIS justify the increased power usage. Additionally, evaluating whether a proposed optimization method can be effectively applied to active RIS involves considering the method's assumptions about the RIS model and its adaptability to incorporate active component characteristics. This ensures the method remains relevant and effective in optimizing RIS-aided systems, regardless of the specific RIS technology employed.

Our work uses passive RIS. For passive RIS, the approach optimizes the phase shift and amplitude of reflected signals within power and data rate constraints, taking into account double path fading. Our technique is limited by RIS power reservation and energy harvesting.

For adapting our approach from passive to active RIS, the solution must be inherently flexible to accommodate various RIS architectures. Since the initial algorithm was designed specifically for passive RIS, only minor modifications are required to fully leverage active RIS's capabilities. Active RIS, distinct from passive versions, supports signal amplification, necessitating adjustments to our optimization techniques. Additionally, by eliminating the constraints associated with power harvesting, active RIS improves the data rate, mitigates power loss, and obviates the need to reserve computational power. These enhancements necessitate a strategic revision to optimize performance effectively.

2) CHANNEL PREDICTION IN MMIMO SYSTEMS

The advancements in massive Multiple Input Multiple Output (mMIMO) systems have been a pivotal cornerstone in modern wireless communication. Research [8] makes it evident that a critical challenge faced in efficiently operating these systems is their inherent complexity and the need for accurate channel state information (CSI) prediction. Traditional methods were often limited by either computational costs or prediction inaccuracies. However, adopting Recurrent Neural Networks (RNNs) for this task has proven transformative. RNNs, by their design, are particularly adept at processing sequences or time series data, allowing them to model and predict the temporal dependencies inherent in wireless channels. Channel responses in mMIMO systems are indeed highly temporally correlated, and treating them as time series data offers predictive advantages. The novelty introduced by the research in [9] highlights the efficacy of RNN-based CSI prediction and introduces a cost-effective mMIMO RNN-based CSI predictor. Furthermore, a comparative study is presented, juxtaposing the computational and economic aspects of RNN-based predictors against traditional CSI predictors, establishing the former's superiority in various performance metrics.

3) ML APPROACHES FOR BEAM STEERING

a: LSTM (LONG SHORT-TERM MEMORY) NETWORK

LSTM represents a significant leap in the evolution of neural architectures tailored for sequence processing tasks. LSTMs, belonging to the family of recurrent neural networks (RNNs), have garnered widespread recognition due to their unparalleled ability to capture long-term dependencies in sequences by leveraging a unique internal state regulated by meticulously designed gates [10]. The architecture revolves around the cell state, an information highway that runs straight down the entire chain. LSTM units maintain a state throughout data processing and consist of three key gates: the input gate, the forget gate, and the output gate, controlling the flow of information (as shown in Equations 1-6). Given an input sequence $\mathbf{x} = (\mathbf{x}_1, \mathbf{x}_2, \ldots, \mathbf{x}_t)$, the LSTM updates its cell state $\mathbf{C}_t$ and hidden state $\mathbf{h}_t$ using:

$$\mathbf{i}_t = \sigma(\mathbf{W}_{ii}\mathbf{x}_t + \mathbf{b}_{ii} + \mathbf{W}_{hi}\mathbf{h}_{t-1} + \mathbf{b}_{hi}) \quad (1)$$

$$\mathbf{f}_t = \sigma(\mathbf{W}_{if}\mathbf{x}_t + \mathbf{b}_{if} + \mathbf{W}_{hf}\mathbf{h}_{t-1} + \mathbf{b}_{hf}) \quad (2)$$

$$\mathbf{g}_t = \tanh(\mathbf{W}_{ig}\mathbf{x}_t + \mathbf{b}_{ig} + \mathbf{W}_{hg}\mathbf{h}_{t-1} + \mathbf{b}_{hg}) \quad (3)$$

$$\mathbf{o}_t = \sigma(\mathbf{W}_{io}\mathbf{x}_t + \mathbf{b}_{io} + \mathbf{W}_{ho}\mathbf{h}_{t-1} + \mathbf{b}_{ho}) \quad (4)$$

$$\mathbf{c}_t = \mathbf{f}_t \odot \mathbf{c}_{t-1} + \mathbf{i}_t \odot \mathbf{g}_t \quad (5)$$

$$\mathbf{h}_t = \mathbf{o}_t \odot \tanh(\mathbf{c}_t) \quad (6)$$

where:

- $\mathbf{i}_t, \mathbf{f}_t, \mathbf{g}_t, \mathbf{o}_t$: Input, forget, cell, and output gate values.
- $\mathbf{h}_t, \mathbf{c}_t$: Hidden and cell state at time t.
- $\mathbf{W}$, $\mathbf{b}$: Weight matrices and bias terms.
- σ: Sigmoid activation function.
- $\odot$: Element-wise multiplication.

Thus, it is an architecture of RNNs adept at handling sequences by retaining long-term dependencies and bypassing the vanishing gradient problem inherent in traditional RNNs.

b: BLSTM (BIDIRECTIONAL LSTM) NETWORK

The BLSTM builds upon the foundational principles of the LSTM by introducing a dual-directional approach. It comprises two LSTMs: one processes the sequence from start to end, while the other processes it in reverse. This bidirectional perspective provides an enhanced understanding of the sequence, integrating past and future contexts when making predictions at any given time step [11]. The architecture can be visualized as two layers of LSTMs: a forward layer and a backward layer. The forward layer reads the sequence in the typical chronological order, while the backward layer reads it in reverse. This influences each time step's output by preceding and succeeding sequence elements (as shown in Equations 7-9). Given an input sequence, the BLSTM computes the hidden states using:

$$\overrightarrow{h_t} = \text{LSTM}_{forward}(\mathbf{x_t}, \overrightarrow{h_{t-1}}) \quad (7)$$

$$\overleftarrow{h_t} = \text{LSTM}_{backward}(\mathbf{x_t}, \overleftarrow{h_{t+1}}) \quad (8)$$

$$\mathbf{h_t} = [\overrightarrow{h_t}; \overleftarrow{h_t}] \quad (9)$$

where:

- $\overrightarrow{h_t}$, $\overleftarrow{h_t}$: Hidden states of forward and backward LSTMs.
- $\mathbf{h_t}$: Concatenation of forward and backward hidden states.

So, it is an extension of LSTM; it processes sequences from both past-to-future and future-to-past orientations, offering enhanced insights for certain sequences.

c: RNN (RECURRENT NEURAL NETWORK)

The RNN stands as one of the pioneering architectures designed for sequence processing. Introducing loops for information persistence, RNNs are naturally suited for tasks where sequential data is processed over time steps, capturing the temporal dynamics of such data [12]. The core idea behind RNNs is incorporating a hidden state, capturing information about previous time steps. This state acts as a memory, passed along through time steps while being combined with the current input (as shown in Equations 10-11). An RNN updates its hidden state using the following:

$$\mathbf{h_t} = \sigma(\mathbf{W_{hh}h_{t-1}} + \mathbf{W_{xh}x_t} + \mathbf{b_h}) \quad (10)$$

$$\mathbf{y_t} = \mathbf{W_{hy}h_t} + \mathbf{b_y} \quad (11)$$

where:

- $\mathbf{x_t}$: Input at time-step t.
- $\mathbf{h_t}$: Hidden state at time-step t.
- $\mathbf{W_{hh}}, \mathbf{W_{xh}}, \mathbf{W_{hy}}$: Weight matrices.
- $\mathbf{b_h}, \mathbf{b_y}$: Bias terms.
- σ: Activation function.

So, it is intrinsically designed for sequential data. RNNs preserve information through their internal loops.

d: RNN-BLSTM NETWORK

The RNN-BLSTM network is a sophisticated architecture incorporating bidirectional layers and enhancing the traditional LSTM structure. This model processes past and future sequence information dynamically. By introducing recurrent connections in the hidden layers, it attempts to revisit past layer computations to refine its current understanding [13]. The RNN-BLSTM can be visualized in two stages: the outer processing stage, where input data undergoes initial processing through bidirectional layers, and the inner LSTM unit operation, where each LSTM cell is a conglomeration of various gates that regulate the flow of information (as shown in Equations 12-13). The iterative refinement process is governed by:

$$\mathbf{h_t^l} = \sigma(\mathbf{W_l h_t^{l-1}} + \mathbf{U_l h_{t-1}^l} + \mathbf{b_l}) \quad (12)$$

$$y_t = \text{softmax}(\mathbf{W_{output}} \mathbf{h_t^L}) \quad (13)$$

where:

- $\mathbf{h_t^l}$: State of layer l at iteration t.
- $\mathbf{W_l}, \mathbf{U_l}$: Feedforward and feedback weight matrices.
- $\mathbf{b_l}$: Bias term for layer l.
- σ: Activation function.

Overall, it is a composite model that likely blends the capabilities of standard RNNs with BLSTM, accentuating bidirectional attributes atop the recurrent features of RNNs.

e: FEEDBACK DNN

FeedbackDNN integrates the power of feedback connections into traditional deep neural networks. By introducing recurrent connections in the hidden layers, FeedbackDNNs attempt to revisit past layer computations, refining and iteratively improving the current layer's understanding [14], [15]. FeedbackDNNs can be seen as an amalgamation of the depth of DNNs with the temporal dynamics characteristic of RNNs (as shown in Equations 14-15). Given an input x, a FeedbackDNN processes it using:

$$\mathbf{h_t^l} = \sigma(\mathbf{W_l x} + \mathbf{U_l h_{t-1}^l} + \mathbf{b_l}) \tag{14}$$

$$y_t = \text{softmax}(\mathbf{W_{output} h_t^L}) \tag{15}$$

where:

- $\mathbf{h_t^l}$: State of layer l at iteration t.
- $\mathbf{W_l}$, $\mathbf{U_l}$: Feedforward and feedback weight matrices.
- $\mathbf{b_l}$: Bias term for layer l.
- σ: Activation function.

It is a DNN variant with feedback connections, potentially elevating its learning capability.

f: OPTIMIZING BEAM STEERING WITH THE AFOREMENTIONED ML TECHNIQUES

The diverse array of ML techniques tailored for optimizing conventional beam steering each offers unique advantages.

Long Short-Term Memory (LSTM) networks, part of the advanced recurrent neural network architectures, excel in capturing long-term dependencies within sequential data, crucial for applications where sequence processing and memory are essential. This capability is significantly beneficial for beam steering, enabling dynamic predictions and adjustments of beam paths over time based on past data behaviors.

Bidirectional LSTM (BLSTM) networks build upon the capabilities of LSTMs by processing sequences from both forward and backward directions simultaneously. This dual-directional approach enriches the understanding by incorporating insights from both past and future contexts, which can substantially enhance prediction accuracy in beam steering, particularly in dynamically changing environments.

Recurrent Neural Networks (RNNs), the foundational technology behind LSTMs and BLSTMs, maintain a state or memory of previous inputs while processing new data. This allows RNNs to preserve essential temporal information, vital for tasks like beam steering where decisions are heavily dependent on the sequence of past actions.

RNN-BLSTM networks enhance traditional RNN capabilities by combining bidirectional LSTM features. This sophisticated architecture processes both past and future sequence information, allowing for a more comprehensive understanding of the data. The integration of bidirectional attributes atop the recurrent features enhances the model's ability to predict and adjust beam paths with greater accuracy and responsiveness to changes in the environment.

Feedback Deep Neural Networks (Feedback DNNs) integrate traditional deep neural network architectures with feedback connections. These connections allow the network to revisit past computations, refining and enhancing the understanding and processing of input data over iterations. This model's ability to dynamically adapt and learn from previous layers' outputs is particularly useful in beam steering, where it can optimize performance by continuously improving the accuracy of the steering mechanism based on real-time data feedback.

In summary, LSTMs offer robust handling of sequence dependencies crucial for consistent beam steering adjustments; BLSTMs enhance this by providing context from both sequence directions, improving the accuracy of steering decisions; RNNs and RNN-BLSTMs provide the foundational framework enabling these technologies to perform effectively by maintaining critical temporal data across beam steering processes; and Feedback DNNs add a layer of iterative refinement that can adapt to complex environments in beam steering.

B. RELATED WORK ON BEAM MANAGEMENT IN RIS USING ML TECHNIQUES

This section reviews the various approaches reported in the literature related to improving beam management in RISs for channel estimation. Incorporating ML techniques, particularly in the context of RISs, has ushered in a transformative approach to beam management. Specifically, ML models strive to meticulously establish a coherent channel between the RIS and the user equipment (UE). This orchestrated channel is the foundation for further refining beamforming and beam-steering operations, ensuring optimized communication.

Taking a more computational approach, the study described in [16] thoroughly investigates a joint design matrix using Deep Reinforcement Learning (DRL)-based Joint Design. The matrix facilitates the synchronization of transmit beamforming at the base station by utilizing a phase shift matrix. This inquiry focuses on using a deep reinforcement learning (DRL) algorithm. The concept's core is in a sequence of iterative interactions with the environment, employing a trial-and-error approach. The algorithm is guided and adjusted by specified rewards. The numerical analysis validates the proposed methods, showing near-optimal transmit power, extended network coverage, and reduced Access Point (AP) transmit power with more IRS usage. The findings reveal that IRS-aided systems are cost-effective compared to Amplify-and-Forward (AF) relay systems, outperforming conventional massive MIMO systems even with IRS-AP coordination delays. The need for joint optimization in IRS-aided multiuser systems and the advantage of deploying IRS in rich scattering environments for improved multi-user service are also highlighted.

In [17], the authors provide a pair of computationally efficient methods, referred to as efficient methods for RIS Coefficients and Power Allocation, which are designed to determine the phase shift coefficients of a RIS along with an optimal power allocation. These algorithms aim to improve the computing efficiency of the RIS coefficient and power allocation estimation process. The initial algorithm combines the effectiveness of gradient descent with fractional programming to ascertain the RIS's phase coefficients and allocate the transmit power optimally. The second technique relies significantly on sequential fractional programming to carefully adjust the phase shifts of the RIS. Both methods can yield up to 300% higher energy efficiency compared to traditional multi-antenna amplify-and-forward relaying. Additionally, the authors successfully explore energy-efficient designs for both transmit power allocation and phase shifts of the surface reflecting elements, focusing on ensuring individual link budget guarantees for mobile users.

The work reported [18] provides an in-depth analysis of the multi-user multiple-input single-output (MISO) communication environment, specifically focusing on the utilization of MISO Communication Aided by RIS with Imperfect Channel State Information (CSI). A Remote Sensing Information System distinctively enhances the topography of this region. However, it is compromised by the presence of poor CSI. The researchers in this work utilize the existing knowledge of expansive fading statistics at the base station (BS). The pool as mentioned above, is subsequently employed to derive Bayesian minimal mean squared error (MMSE) channel estimates. A crucial stage in this process entails utilizing a carefully selected collection of ideal phase shift vectors by the RIS during many sub-phases of channel estimation. Both empirical and analytical evaluations support the assertion that the resulting mean squared error (MSE) is significantly better, surpassing the MSE obtained from least squares (LS) estimates. Reinforcement Learning (RL) offers dynamic learning capabilities particularly well-suited to RIS systems, which often need real-time adaptation.

Deep learning, a subset of ML, has been instrumental in predicting the optimal configurations of RIS. For instance, the works in [18], [19], [20], and [21] proposed deep learning-based optimization techniques for RIS, showing significant improvements in system performance, particularly in settings with dynamic channel conditions.

The authors in [22] examine how estimating the downlink channel in an RIS-enabled wireless communication system requires substantial pilot overhead. Utilizing ML techniques, particularly neural networks, creates the potential to infer channels requiring fewer pilot signals. Nevertheless, the efficacy of a neural network that has been trained using data from a single user is constrained when it comes to effectively handling a wide range of channel conditions. This work presents an approach utilizing a collaborative neural network, incorporating distributed machine learning (DIML) techniques. Specifically, the network is jointly trained by both the base station and the users. Implementing a layered architecture enhances precision by identifying specific characteristics of communication channels in various situations. Simulation results demonstrate that networks driven by deep machine learning (DEML) outperform networks relying solely on individual user data, leveraging the DEML technique to collaboratively train a downlink channel estimation neural network shared by all users. This neural network can be collaboratively trained by the Base Station (BS) and the users with the help of the DEML technique. So, in this context, the distributed learning technology the paper is using is ''Distributed Machine Learning (DIML)''.

The authors in [23] study investigate the application of ML techniques in the development of receivers for multi-user multiple-input multiple-output (muMIMO) systems supported by RIS. The aim is to overcome the need for intricate channel information requirements. This study examines the potential benefits of utilizing RIS in conjunction with mMIMO technology to enhance data transmission's reliability and energy efficiency. However, constructing receivers for large-scale networks using traditional mathematical approaches requires complex statistical techniques. The Extreme Learning Machine (ELM) is recognized as a highly effective ML technique for MIMO receiver design owing to its shortened learning procedure. However, the effectiveness of its learning process may be compromised due to the arbitrary choice of hidden layer dimensions. To address this issue, the authors proposed the implementation of an incremental EML (I-ELM) based receiver designed explicitly for the RIS-mu-MIMO system. The weights between this innovative receiver's hidden and output layers are determined through an automated process of augmenting hidden neurons based on specific criteria.

In the study [24], the authors introduce an ML methodology to enhance the effectiveness of routing in multi-hop networks by utilizing multiple RIS (M-RIS). This study presents a comprehensive phase model for RIS, which considers the impact of discrete phase shifts on amplitude fluctuations. The objective is to enhance the efficiency of data transmission routes, employ passive beamforming using RIS, and allocate power resources optimally. To address the intricacies of this issue, the authors suggest enhancing the passive beamforming technique in RIS and refining the routing and power allocation strategies. The distributed learning system incorporates a cascade forward backpropagation network within each relay node. The proposed approach effectively addresses the issue of dimensionality encountered in traditional reinforcement learning when applied to RIS optimization. The DCBN (Deep Cascade Neural Network) utilizes a series of interconnected neural networks, establishing connections between channel matrices and RIS coefficients. This framework aims to improve transmission rates by leveraging the backpropagation algorithm for

training purposes. The findings from the Robust Incremental approach indicate that the utilization of the Proximal Policy Optimization (PPO) method, which incorporates clipping, effectively determines the most favorable routing and power solutions within the context of the Markov decision process (MDP).

The authors in [25] introduced a RIS-assisted multi-user downlink system employing both non-orthogonal (NOMA) and orthogonal (OMA) access schemes. They considered the time overhead for RIS setup at the start of each fading channel. They aimed to optimize throughput by adjusting the RIS phase shift and AP's power for each channel block. To address this, they proposed two ML tools: environment-trained deep learning (ETDL) and an exploration attenuated deep determines the policy gradient (EA-DDPG) algorithm. ETDL trains the DL agent directly from the communication environment, removing the need for a training dataset, while EA-DDPG offers continuous control of phase shifts. They viewed the phase shift control as a Markov decision process, addressable with reinforcement learning (RL) through the Bellman equation.

In [26], the authors propose the utilization of a federated learning (FL) methodology, employing a convolutional neural network (CNN) that is trained on individual users' local datasets, hence eliminating the need to transmit the datasets to a central server (BS). Due to its low-complexity nature, ML provides efficient solutions for addressing physical layer design challenges, such as channel prediction. In conventional practice, centralized learning (CL) is employed, wherein data is gathered from users at the base station (BS), resulting in substantial communication overhead. The authors introduce a frequency-domain-based channel estimation technique for both conventional and RIS-assisted large MIMO systems.

The authors in [27] employ RIS technology to tackle the concern that Federated learning (FL) has been offered as a means to leverage extensive data in mobile edge networks, presenting a decentralized ML option. The utilization of over-the-air computation enhances communication efficiency in federated learning by facilitating the concurrent uploading of local models. Nevertheless, the utilization of over-the-air federated learning (FL) is hindered by the ''straggler issue'', which arises from the disparate communication capabilities of edge devices. This issue manifests when the device possessing the weakest channel impedes the pace of model aggregation. The authors analyze the convergence of learning, focusing on a system that involves **PS** and **M** edge devices. The objective of this system is to minimize an empirical loss function. The proposed system encompasses three key components: the dissemination of the current global model, the computation of local gradients, and the utilization of over-the-air computation for federated learning model aggregation. This paper proposes a comprehensive methodology for optimizing the selection of devices, over-the-air transceivers, and RIS phase shifts.

The framework proposed by the authors in [21] introduces the utilization of RIS to support non-orthogonal multiple access (NOMA) downlink transmission. The authors of this study tackle a persistent optimization problem related to NOMA user partitioning and RIS phase shifting. Their objective is to maximize the data rate for mobile users over an extended period. The utilization of a modified object migration automation (MOMA) technique is employed for user partitioning. At the same time, introducing a deep deterministic policy gradient (DDPG) approach is implemented to control the RIS phase. In contrast to conventional approaches, the utilization of a continuous learning model enables the attainment of optimal decisions using both exploration and exploitation. The study's findings indicate that using RIS-aided NOMA demonstrates superior performance compared to standard orthogonal multiple access (OMA) methods. The DDPG algorithm demonstrates proficiency in acquiring knowledge about the distribution of resources over extended periods. 3) Enhanced performance can be attained by optimizing RIS phase shifts.

Finally, The authors in [28] proposed a RIS-assisted Non-Orthogonal Multiple Access (NOMA) Internet of Things (IoT) network. This network incorporates a Quality of Service (QoS)-based NOMA clustering strategy, which aims to enhance the use of wireless resources among IoT devices. The objective is to optimize the throughput by manipulating the RIS's phase shifts and the base station's power. This study aims to compare the performance of deep learning (DL) with deep reinforcement learning (DRL). DL utilizes the model-agnostic-meta-learning (MAML) technique to achieve faster convergence and enhanced generalization. On the other hand, DRL applies the DDPG algorithm to make continuous phase-shift changes. DL optimizes immediate throughput, whereas DRL aims to boost long-term throughput by effectively regulating power usage over time.

1) ML-BASED CHANNEL ESTIMATION FOCUSING SCHEMES

The density and high mobility of connected nodes characterize Modern Wireless communication. For instance, vehicular communication systems present unique challenges due to this high mobility and rapidly varying channel conditions. As indicated by the study in [29], the IEEE 802.11p standard, designed for vehicular communications, faces limitations in its ability to provide accurate channel estimates. The primary cause of this constraint can be attributed to an inadequate allocation of pilot symbols, which play a crucial role in channel estimation. Traditional estimators that conform to this norm experience notable deterioration in performance, especially in cases involving high-speed vehicles. To bridge this existing deficiency, the study presents a novel estimator that leverages the capabilities of Long Short-Term Memory (LSTM) units, which are a specialized variant of Recurrent Neural Networks (RNNs). LSTM models are renowned for effectively retaining and utilizing information on long-term dependencies. Consequently, these models are particularly

suitable for dynamic environments characterized by complex and evolving patterns. Incorporated into the ML-based channel estimation framework is a temporal averaging (TA) processing phase, which serves the purpose of diminishing noise and augmenting the precision of the estimates. This paper presents an analytical assessment of noise mitigation, emphasizing the crucial significance of TA processing. The simulation findings support the assertion that the proposed estimator is superior, as it demonstrates its improved performance compared to previous deep learning-based approaches and emphasizes its optimal computing efficiency.

Moreover, Recent advancements in wireless communication have highlighted the pivotal role of ML, particularly Long Short-Term Memory (LSTM) networks, in enhancing system performance. Authors in [30] introduce a sophisticated decision-making system built upon LSTM, specifically designed to tackle the dynamic nature of wireless network data. This ingenious approach is devised to navigate through the intricate landscape of channel conditions, thereby rendering a more efficient and reliable communication system. The system's design pivots on harnessing the capabilities of RIS to maximize energy harvesting, thereby amplifying the overall energy efficiency of wireless communications. In essence, RIS is a programmable environment modifier, allowing for optimal modulation of wireless conditions to bolster communication standards. The primary objective of the LSTM model, as proposed in the study, is to ascertain the optimal RIS configuration tailored to individual transmissions. The model undergoes rigorous training in a real-time context to achieve this precision, assimilating the dynamic variances inherent in real-world wireless scenarios. These transmissions intend to cater to users dispersed throughout diverse regions within the encompassed wireless network. The study incorporates the LSTM network into an RIS-aided downlink system model for empirical validation, further enhanced using the Adam optimizer. The Adam optimizer, renowned for its efficiency in stochastic optimization, complements the LSTM's potential, making the system adept at adapting to intricate channel conditions. The dual metrics under examination were the system's energy conservation capability and robustness against varied external challenges. Through extensive simulations, the model showcased exemplary outcomes. A paramount finding was the pronounced increment in energy efficiency, which surged to an impressive 35.42% upon augmenting the RIS components from a base of 9 to 25. This enhancement signifies a substantial reduction in energy consumption as compared to traditional counterparts. Concurrently, the system didn't compromise on transmission speed, registering a commendable net data rate surpassing 100 bps/Hz, thereby affirming its potential to facilitate swift data transmission while conserving energy.

The study by [31] explores a novel approach to transmission design in RIS-aided multiuser networks. The authors propose utilizing long-term Channel State Information (CSI) to reduce the significant overhead associated with channel estimation. The core of their methodology is the adoption of a deep deterministic policy gradient (DDPG) algorithm, which is pre-trained using channel vector information to optimize the system's transmission design. Their simulation results indicate that this long-term CSI-based design surpasses conventional instantaneous CSI-based strategies, offering a more efficient net throughput when considering the reduced channel estimation overhead.

Conversely, [32] addresses the challenges of beam training within extremely large-scale RIS in near-field scenarios. They recognize the heightened pilot overhead intrinsic to near-field models and many candidate codewords. Their response is a deep learning-based training scheme that utilizes deep residual networks for codeword estimation, which is shown to reduce pilot overhead drastically while retaining performance efficacy. The paper discusses two distinct schemes: a far-field beam-based scheme and a partial near-field beam-based scheme, with the latter emphasizing reduced pilot overhead by focusing only on a subset of codewords. The authors also introduce an improved variant of the partial scheme that leverages the neural network's predictive capabilities to enhance performance further. Their findings demonstrate a remarkable potential in overhead reduction, by approximately 95%, through their proposed beam training schemes.

2) EVALUATION OF THE LITERATURE REVIEW

Extensive research, such as the work by Wu and Zhang [16], highlights the use of Deep Reinforcement Learning (DRL) in enhancing remote sensing image analysis technologies to RIS in order to examine the beam. Huang et al. [17] offer a different perspective emphasizing phase shift and power allocation in RIS-aided systems. Deep learning optimization for RIS, as shown by Yang et al. and Huang et al. [18], [21], aligns with the collaborative neural network approach of Dai and Wei [22]. Both papers explore the dynamic nature of wireless channels but focus on different aspects. Huang et al.'s study [18] on MISO communication complements the findings of Liu et al. [27] and Yang et al. [21], emphasizing the need for real-time adaptation in RIS systems. Distinct approaches to RIS receiver design are presented by Mahmood et al. [23] and Huang et al. [17], highlighting the varied focus on reconfigurability and phase shift coefficients. Optimization using ML is central to the works of Huang et al. [24] and Zhong et al. [25], but the former delves into multi-hop networks while the latter looks at multi-user downlink systems. Elbir and Coleri [26] and Gupta et al. [30] both target channel estimation in MIMO systems using ML, offering unique methodologies. Zou et al. [28] and Yang et al. [21] discuss NOMA in RIS but employ different machine-learning strategies. In vehicular communication, Gizzini et al. [29] introduces an LSTM-based estimator, a perspective also explored by Gupta et al. [30] in the RIS configuration context. The study by [31] introduces a novel transmission design approach for RIS-aided multiuser networks that leverages long-term Channel State

TABLE 1. Comparative analysis of ML-based RIS beam management techniques.

Reference	Technique	Objective	Advantages	Limitations
Our Approach	FeedbackDNN with 64QAM	Optimize RIS beamforming for energy efficiency	Superior accuracy and performance in high mobility scenarios. Reduced pilot overhead.	Requires initial extensive training data.
[16]	DRL-based Joint Design	Synchronize transmit beamforming with phase shift matrix	Improved network coverage with reduced AP transmit power.	May not adapt quickly to rapidly changing environments.
[17]	Efficient Methods for RIS Coefficients and Power Allocation	Determine phase shift coefficients and optimal power allocation	Up to 300% higher energy efficiency compared to traditional methods.	Computational complexity for real-time implementation.
[18]	MISO Communication Aided by RIS with Imperfect CSI	Enhance MISO communication with Bayesian MMSE	Reduced MSE in channel estimation.	Dependent on the accuracy of prior fading statistics.
[22]	Collaborative Neural Network	Estimate downlink channel with fewer pilots	Improved performance leveraging DML.	Performance varies with the range of channel conditions.
[32]	Deep Learning-Based Training for Large-Scale RIS	Reduce pilot overhead in beam training	Drastic reduction in pilot overhead while retaining performance.	Focused primarily on near-field scenarios.
[19], [20], [18], [21]	Deep Learning Optimization for RIS	Optimize RIS configurations for dynamic channel conditions	Significant improvements in system performance.	Requires extensive computational resources for training.
[23]	EML Techniques for RIS-mu-MIMO Systems	Design efficient receivers for muMIMO systems	Overcomes intricate channel information requirements.	Effectiveness depends on the choice of hidden layer dimensions.
[24]	ML Methodology for Multi-hop Networks with M-RIS	Enhance routing efficiency using RIS	Improves data transmission rates and energy efficiency.	Complexity in implementing the cascade forward backpropagation network.
[25]	RIS-assisted Multi-user System with ML Tools	Optimize throughput with RIS phase shift control	Balances throughput optimization with time overhead.	Challenging to implement in highly dynamic environments.
[26]	Federated Learning for Channel Estimation	Efficient channel prediction without central data collection	Lowers communication overhead for channel estimation.	Limited by the local datasets' diversity and size.
[27]	Over-the-Air Computation for FL in RIS systems	Enhance FL efficiency with RIS technology	Addresses the straggler issue in FL model aggregation.	Depends on the optimization of RIS phase shifts for efficiency.
[21]	RIS-aided NOMA with DDPG	Maximize user data rate over time	Outperforms OMA methods. Optimal RIS phase control.	Requires balance between exploration and exploitation.
[28]	RIS-assisted NOMA IoT Network with QoS-based Clustering	Optimize throughput and resource use among IoT devices	Utilizes DL and DRL for efficient phase shift control.	Differentiates between immediate and long-term throughput optimization.
[29]	LSTM for Channel Estimation in Vehicular Communications	Address high mobility challenges in vehicular networks	Superior performance with reduced noise and enhanced precision.	Tailored mainly for high-speed vehicular scenarios.
[30]	LSTM Network for Dynamic Wireless Network Data	Maximize energy harvesting in wireless communications	Significant increase in energy efficiency and data rate.	Training requires real-time context adaptation.
[31]	Long-Term CSI-Based Design with DDPG	Reduce channel estimation overhead	More efficient net throughput with reduced overhead.	Predominantly advantageous in long-term operation scenarios.

Information (CSI), employing a deep deterministic policy gradient (DDPG) algorithm. This methodology aims to optimize system transmission design more efficiently than traditional methods relying on instantaneous CSI. In [32], on the other hand, the author proposes a deep learning-based training scheme for beam training in large-scale RIS, particularly in near-field scenarios. This approach significantly reduces pilot overhead by approximately 95% while maintaining performance, emphasizing efficiency and the potential of deep learning in optimizing RIS systems. In summary, these studies underscore the advancements in RIS technology, highlighting the potential of ML and deep learning techniques in the field.

3) COMPARISON OF THE LITERATURE REVIEW INVESTIGATED APPROACHES WITH OURS

In our investigation of ML techniques for enhancing beam management in RIS, we have meticulously compared our approach, which leverages a FeedbackDNN with 64QAM, against a spectrum of state-of-the-art methodologies as detailed in Table 1. Our methodology stands out for its ability to optimize RIS beamforming for energy efficiency,

demonstrating superior accuracy and performance, especially in high mobility scenarios. This is achieved with a reduced pilot overhead, although it necessitates initial extensive training data. Comparatively, the Deep Reinforcement Learning (DRL)-based Joint Design by Wu and Zhang [16] and the Efficient Methods for RIS Coefficients and Power Allocation by Huang et al. [17] focus on improving network coverage and energy efficiency through optimal power allocation and phase shift coefficients determination, respectively. However, these approaches may face challenges in rapidly changing environments and bear computational complexities.

Further, the work by Huang et al. [18] on MISO Communication Aided by RIS with Imperfect CSI, and the Collaborative Neural Network introduced by Dai aand Wei [22], show advancements in channel estimation and downlink channel estimation with fewer pilots, leveraging Bayesian MMSE and Distributed Machine Learning (DIML). These techniques, while improving performance, depend on the accuracy of prior fading statistics and vary with the range of channel conditions. Deep Learning-Based Training for Large-Scale RIS by Liu et al. [32] addresses pilot overhead in beam training, achieving a drastic reduction in pilot overhead. This method, like ours, emphasizes efficiency and the potential of deep learning in optimizing RIS systems, albeit with a primary focus on near-field scenarios.

The extensive comparison reveals that while each investigated approach contributes significantly to the advancement of RIS beam management, our FeedbackDNN with 64QAM approach distinguishes itself by offering a balanced trade-off between high accuracy, reduced pilot overhead, and adaptability to high mobility scenarios, setting a new benchmark for optimized communication. This comparative analysis, grounded in the meticulous evaluation presented in Table 1, underscores the transformative potential of integrating ML with RIS technologies, heralding a new era of optimized wireless communication systems.

III. SYSTEM DESIGN AND OPTIMIZATION PROCESS

A. SYSTEM DESCRIPTION

The proposed system capitalizes on the profound learning ability of Feedback DNN to accurately predict the channel conditions to effectively and efficiently manage the beams from an RIS and elevate the overall wireless performance in vehicular networks. More specifically, the aim is to employ an ML model to predict the optimal reflecting signal characteristics anchored on the *"HLS Structure"* or *"Hybrid Learning Structure Structure"* (as shown in Section IV-B2) – the input signal directed towards the RIS. Harnessing these predictions, the objective is to dynamically craft the ω array via the referenced equation, thereby achieving superior communication.

Delving deeper into this setup, we envision a system comprising of (as shown in Figures 1 and, 2): (1) The Base Station (BS) with M antennas, (2) Receivers each equipped with a single antenna, and (3) a RIS with N elements. In locations without a line of sight between the BS and the user, the RIS, typically mounted on surrounding structures, bridges this communication gap. This intelligent surface comprises dynamic components controlled by a dedicated controller at the BS, negating the need for a direct transmission link. A pivotal aspect of this system is its energy efficiency. Derived from energy-harvested sources and self-powered RIS reflectors, it exemplifies sustainable communication. Given the unpredictability of energy sources, an Energy Storage Model (ESM) is integrated. Notably, the RIS conserves energy regardless of its components' states. It calculates power consumption based on its components, ensuring energy is optimally used. This system's multifaceted relationship between energy conservation, transmission power, achievable data rates, and received signal energy complicates optimization. Here, a Deep Learning (DL) methodology can assist. Recognizing the problem's non-linearity, an approach using ML, i.e., Feedback DNN, is proposed. By inputting parameters like transmission power and user-device spatial dynamics, the model aims to maximize energy conservation. This study concentrates on a downlink system model where a single RIS plays a central role in mediating communication between a base station (BS) and multiple receivers.

B. SIGNAL MODEL AND PROBLEM FORMULATION

Transmission Dynamics at the Base Station (BS):At the BS, the transmitted signal, x, can be defined as in Equation 16 [33], [34].

$$x = \mathbf{W} \times \mathbf{s} \tag{16}$$

where:

- $\mathbf{W} \in \mathbb{Z}^{M \times K}$ is the linear precoding matrix where M is the total number of BS antenna elements and K is the number of data symbols transmitted.

$$\text{BS Antenna Elements} \downarrow \quad \text{Data symbols} \rightarrow \quad \begin{pmatrix} \mathbf{w_{1,1}} & \mathbf{w_{1,2}} & \cdots & \mathbf{w_{1,K}} \\ \mathbf{w_{2,1}} & \mathbf{w_{2,2}} & \cdots & \mathbf{w_{2,K}} \\ \vdots & \vdots & \ddots & \vdots \\ \mathbf{w_{M,1}} & \mathbf{w_{M,2}} & \cdots & \mathbf{w_{M,K}} \end{pmatrix}$$

- $\mathbf{s} = (s_1, s_2, \ldots, s_K)^T$ is a vector that represents the unit power transmitted data symbols with zero mean, unit variance, and mutual independence properties.

The power constraint is represented by Equation 17.

$$\text{tr}(\mathbf{W}^H \times \mathbf{W}) \leq T_{max} \tag{17}$$

where tr() is the Matrix trace function and $\mathbf{W}^H$ is the Matrix conjugate transpose, also known as the Hermitian transpose.

- T_{max}: Maximum transmission power.

1) SIGNAL PROPAGATION TO THE RIS

As the signal moves between the BS and the RIS, it's modulated by the BS-R channel state information. Thus, the

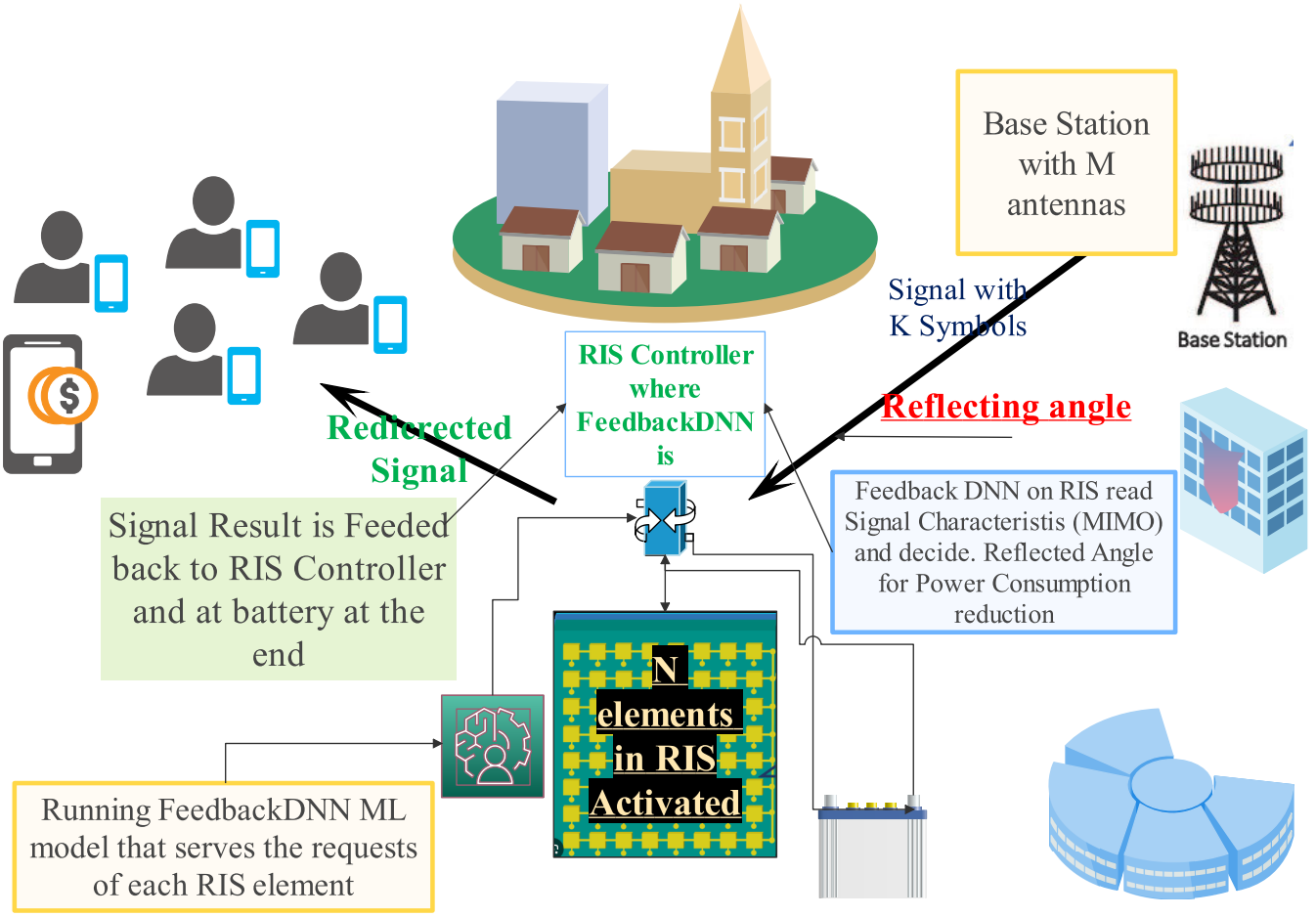

FIGURE 1. The system architecture.

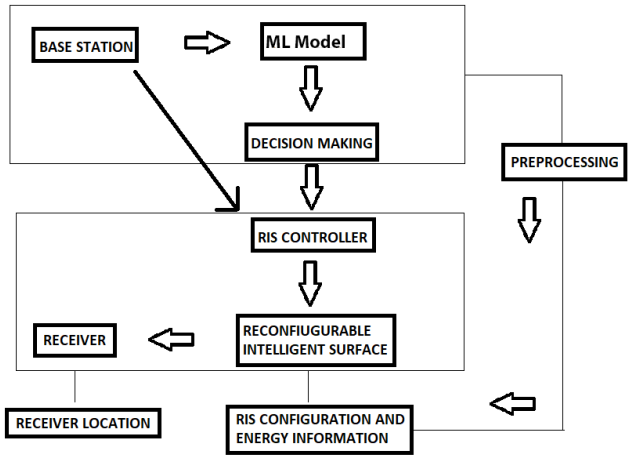

FIGURE 2. The system components architecture.

signal at the RIS is shown in Equation 18.

$$y = \mathbf{A} \times x \tag{18}$$

where:

- $\mathbf{A} \in \mathbb{Z}^{N \times M}$ is the channel state information from the BS to the RIS, and N is the number of RIS elements.

2) SIGNAL RECEPTION AT THE USER'S END

The received signal, r, combines transformations, including channel modulations and phase shifts from the RIS elements. So, the RIS phases each component of this received signal before relaying it to the users. The final received signal at the user is then shown in Equation 19.

$$r = \mathbf{F} \times \omega \times \mathbf{A} \times \mathbf{W} \times \mathbf{s} + \mathbf{u} \tag{19}$$

where:

- $\mathbf{F} \in \mathbb{Z}^{K \times N}$ is the channel state information between RIS and the users.
- $\omega = \text{diag}(\mathbf{w})$ where $\omega_n = e^{j\theta_n}$ is the phase shift at the n^{th} antenna element of RIS. $\theta \in (0, 2\pi)^N$.
- $\mathbf{u}$ represents complex Gaussian noise with zero mean and variance γ^2.

To further process the received signal, it's scaled by $\mathbf{C}$ as in Equation 20.

$$s_c = \mathbf{C} \times r \tag{20}$$

where $\mathbf{C} = \text{diag}(c_1, c_2, \ldots, c_K)$, is the scaling coefficients vector which is used to compensate for channel distortions, noise mitigation, or other signal processing goals. In our case, we employ neural networks and, more specifically,

deep learning models to derive these coefficients based on historical data and through a brute-force investigation of all the parameters that can affect the signal from RIS toward the UE and the current state of the received signal.

The spectral efficiency, indicative of the system's performance, improves with a higher Signal-to-Interference Noise Ratio (SINR). Using the above expressions, the total system rate for a RIS-enabled MIMO system can be expressed as in Equation 21.

$$R = \sum_{k=1}^{K} \log_2(1 + \tau_{\mathbf{k}}) \tag{21}$$

where:

- R: Represents data rate (in bits per second) per unit bandwidth. It encapsulates the efficiency of the available bandwidth for data transmission, especially when considering interference and noise.
- $\tau_{\mathbf{k}}$: The k^{th} SINR value.

Practically, the above equation computes the cumulative spectral efficiency across K users or channels.

To enhance user experience, maximizing the data rate is essential, with the RIS beam's angle playing a crucial role. This demands a data rate maximization formulation as in Equation 22 [33], [34].

$$\max_{\theta} R(\theta) = \log_2\left(1 + \frac{|\mathbf{h}_{\text{RIS-UE}}(\theta)|^2 \mathbf{P}}{\sigma^2}\right) \tag{22}$$

Subject to $0 \leq \theta \leq \Theta_{\max}$

The formula presented describes an optimization problem related to maximizing the data rate function $R(\theta)$ in a RIS-enabled wireless environment where:

- θ represents the phase shift introduced by the RIS. It is a key variable in the optimization problem, affecting the communication rate between the RIS and the UE. The value of θ directly influences the channel gain $|\mathbf{h}_{\text{RIS-UE}}(\theta)|^2$, signifying the dependency of the communication link's quality on the chosen phase shift.
- $\Theta_{\max}$ denotes the upper bound on the phase shift that the RIS can introduce and ensures that θ remains within operationally defined or physically feasible bounds.
- $|\mathbf{h}_{\text{RIS-UE}}(\theta)|^2$: This denotes the squared magnitude of the channel gain between the RIS and UE, which depends on the phase shift θ.
- $\mathbf{h}_{\text{RIS-UE}}(\theta)$: This vector represents the complex channel coefficients describing the path from the Reconfigurable Intelligent Surface (RIS) to the User Equipment (UE).
- $|\mathbf{h}_{\text{RIS-UE}}(\theta)|^2$: This denotes the squared magnitude of the channel gain between the RIS and UE, which depends on the phase shift θ. The squared magnitude, $|\mathbf{h}_{\text{RIS-UE}}(\theta)|^2$, reflects the power gain of the channel as a function of the phase shift θ applied by the RIS. It illustrates how effectively the RIS can focus or steer the signal towards the UE, enhancing signal reception under varying phase shift conditions.
- $\mathbf{P}$: This represents the transmitted power.
- σ^2: This is the variance of the channel's additive white Gaussian noise (AWGN), representing the noise power.

RIS consists of many passive elements that can introduce phase shifts to the incident signals. By optimizing these phase shifts, it's possible to constructively combine signals at the desired receiver, thereby enhancing the communication rate or coverage. The optimization problem aims to maximize the communication rate between the RIS and UE by appropriately tuning the phase shift θ while ensuring it remains within certain bounds.

Note that the system is powered by energy harvested from sources like solar panels, integrated with an Energy Storage Model (ESM). The RIS reflectors can utilize this harvested energy for signal propagation. Reflecting elements on the intelligent surface can be dynamically activated or deactivated, optimizing energy efficiency.

The role of the Base Station (BS) in this setup is critical. It actively adjusts its configurations based on the predictions these models generate. The Mean Squared Error (MSE) is a vital metric in this process. The BS aims to minimize this error across all training samples by comparing the predicted results with the actual ones. In terms of signal transmission, the system is set up such that the number of antennas broadcasting the signal matches the number of "Total Used Subcarriers" that OFDM supports.

For the ML models in use, the input, denoted as x, comprises features such as the signal characteristics that are transmitted by the MIMO antenna on the BS combined with the locations of both the BS and User Equipment (UE). In contrast, the output, marked as y, serves as a training target. This target encapsulates the optimal signal characteristic, considering factors like the required SNR, and mobility (with an emphasis on high mobility, given that the UE's destination coordinates are defined by its starting position. Note that the MIMO BS and RIS possess stationary positions, devoid of any velocity, concerning their respective coordinates.), channel_model (VTV), modulation_order (SDWW_QPSK), and scheme (DPA_TA).

Our methodology also involved conducting a brute force simulation using MATLAB® paired with the 5G toolkit. Based on the chosen SNR and other parameters, the best signal characteristics for given locations are pinpointed, referred to as the true channel structure. It's essential to note that the choices made during this phase correspond to a specific ω array. The overarching goal of the ML approach is to make accurate predictions about the optimal reflecting signal characteristics as they hinge on the "HLS Structure", which is the input signal directed towards the RIS. The culmination of this process is constructing the desired signal by accurately computing the ω array.

Given equation 19 and assuming $\mathbf{A} \times \mathbf{W} \times \mathbf{s}$ is represented as $\mathbf{B}$, the equation can be re-written as in Equation 23.

$$r - \mathbf{u} = \mathbf{F} \times \omega \times \mathbf{B} \tag{23}$$

If $\mathbf{F}$, $\mathbf{A}$, $\mathbf{W}$, and $\mathbf{s}$ are known and $\mathbf{B}$ is a column vector, one can naively express ω as in Equation 24.

$$\omega = \mathbf{F}^{-1} \times (r - \mathbf{u}) \times \mathbf{B}^{-1} \tag{24}$$

However, this solution poses challenges:

1) The matrix $\mathbf{F}$ might not be invertible.
2) The product $(r - \mathbf{u}) \times \mathbf{B}^{-1}$ may not be meaningful depending on the dimensions of $r - \mathbf{u}$ and $\mathbf{B}$.
3) The matrix ω is a diagonal matrix representing phase shifts, but the solution does not guarantee a diagonal matrix or the specific structure of $\omega_{\boldsymbol{n}}$.

Given the structure of ω, optimization approaches might be more suitable to determine the values in ω based on some objective or criteria.

C. ENERGY CONSUMPTION PARADIGM

The communication system under consideration primarily relies on energy harvested from ambient sources, emphasizing the utilization of self-sustaining energy practices. One of the highlights of this system is the deployment of self-powered RIS reflectors. These reflectors can harness energy directly from environmental sources, most notably through solar panels. This energy-harvesting model addresses the inherent unpredictability associated with ambient energy sources, requiring an adaptive energy storage model (ESM) to manage the collected energy. The ESM is crucial in ensuring that the RIS adopts a reflection strategy that balances energy availability and the demand of ongoing communication tasks. Consequently, the system allows for real-time control over the RIS components. Specifically, these controls regulate the RIS elements' dynamic ON/OFF status, which in turn impacts the phase shift imparted on transmitted signals. Such fine-grained control is pivotal in enhancing the system's overall energy efficiency, ensuring optimal performance without excessive energy expenditure.

1) THE ENERGY CONSUMPTION OF THE SYSTEM

The energy consumption of the system is modeled as in Equation 25 [33], [34].

$$SU_t = PRIS_t \times \delta \tag{25}$$

where:

- $PRIS_t = \sum_{n=1}^{N} \rho_t \times T_b$
- ρ_t: Represents the activation level or state of the t^{th} RIS phase shifter. Its value is multiplied by the power consumption T_b of a b-bit resolution phase shifter to determine the total power consumed by that particular phase shifter during its operation. The sum across all phase shifters gives the RIS's total power consumption $PRIS_t$ during the transmission duration δ, which is binary and takes the value 0 for OFF and 1 for ON.
- T_b: Power consumption of a b-bit resolution phase shifter.
- δ: Transmission duration.

The saved energy is as shown in Equation 26.

$$SE_t = \min(\mathbf{SE_{t-1}} - \mathbf{SU_{t-1}} + \beta_{\mathbf{t-1}}, \mathbf{E_{max}}) \tag{26}$$

where:

- $\mathbf{SE_{t-1}} \geq 0$: Represents the stored energy at the previous transmission time.
- $\mathbf{SU_{t-1}}$: Denotes the energy consumed by the RIS elements during the previous transmission.
- $\beta_{\mathbf{t-1}}$: Energy harvested at the previous transmission time. This energy can be harvested from various external sources, such as ambient RF (radio frequency) signals, solar energy, or other renewable sources.
- $\mathbf{E_{max}}$: System Maximum energy storage capacity.

To compute the energy harvested by the system at the previous transmission time, $\beta_{\mathbf{t-1}}$, from the saved energy equation, we can rearrange and get:

$$\beta_{\mathbf{t-1}} = \mathbf{SE_t} + \mathbf{SU_{t-1}} - \mathbf{SE_{t-1}} \tag{27}$$

The above formulation computes the harvested energy at the previous transmission time by accounting for the change in stored energy and the energy consumed during the last transmission. It gives the energy harvested by the system, assuming that the saved energy $\mathbf{SE_t}$ does not reach the maximum storage capacity $\mathbf{E_{max}}$.

Due to its non-linearity, achieving energy conservation while ensuring efficient communication presents an optimization challenge. Traditional approaches often fail to address this complexity, leading us to turn to Deep Learning techniques. Among the techniques well-suited for this task are models tailored for sequential data prediction, including LSTM, BLSTM, RNN_BLSTM, RNN, and FeedbackDNN.

D. OPTIMIZATION PROBLEM BASED ON THE DESCRIBED SYSTEM

From a systems optimization perspective, the primary objective is to enhance energy conservation during downlink transmission. Achieving this goal requires a multifaceted approach, encompassing adjusting the base station's transmission power, fine-tuning the RIS's phase shifts, and judiciously determining the RIS elements' operational status. The nested optimization problem can be expressed as in Equation 28.

$$\max_{\mathbf{T_p}, \omega, \rho} \min_{t} \mathbf{FO_t}(\mathbf{T_p}, \omega, \rho) \tag{28}$$

Such as

$$\sum_{t} \mathbf{T_p} < \mathbf{T_{max}}$$

$$\mathbf{SU_t} \leq \mathbf{SE_t} \; \forall \; \textit{transmission at time } t$$

The first constraint concerns maintaining the total transmission power below the maximum allowable transmission power. The second constraint also represents the energy consumption of the RIS element during each transmission,

which must be lower than the overall conserved energy determined by the energy harvested formula presented in Equation 27. Equation

$$\mathbf{FO_t} = t_r\{\mathbf{F} * \omega * \mathbf{A} * \mathbf{W} * \mathbf{W}^H * \mathbf{A}^H * \omega^H * \mathbf{F}^H\} + \gamma^2 * \mathbf{K},$$

estimates the energy conservation during a transmission measured as the energy of the received signal. In addition, ρ is used for assessing achievable data rates. Also $\mathbf{T_p}$ denotes the transmission power. More specifically, the given mathematical expression represents a nested optimization problem where the total harvested energy utilized by the BS for decision-making to achieve energy efficacy is obtained by maximizing the minimum of the conserved power in each transmission. A detailed breakdown is the following:

Optimization Problem Explanation:

- $FO_t(\mathbf{T_p}, \omega, \rho)$: This function encapsulates the entire system's performance at a given time t and is influenced by the parameters the Base Station transmission power $\mathbf{T_p}$, the RIS's phase shifts ω and the operational status of the RIS elements ρ. While the exact nature of this function is context-dependent, its structure indicates its dependency on these parameters.
- $\min_t$: This is a minimization operation concerning the variable t, aiming to identify the system's most vulnerable scenario — essentially when FO_t attains its minimum value for the set parameters.
- $\max_{\mathbf{T_p},\omega,\rho}$: Having identified the worst-case scenario through the minimization, this maximization seeks to optimize $\mathbf{T_p}$, ω, and ρ such that this "worst-case" performance is as optimal as possible, ensuring that the system is both efficient and resilient.

Interpretation: The nested optimization problem can be thought of as a two-step procedure:

- For fixed values of $\mathbf{T_p}$, ω, and ρ, find the value of t that minimizes $FO_t(\mathbf{T_p}, \omega, \rho)$.
- Then, among all these minimum values (for different combinations of $\mathbf{T_p}$, ω, and ρ), find the combination of $\mathbf{T_p}$, ω, and ρ that results in the maximum of these minimum values.
- This type of problem is often seen in scenarios where there's a need to ensure the worst-case performance (captured by the inner minimization) is as good as possible (captured by the outer maximization).

Our approach aims to optimize simulations to attain the highest possible values for achieving a particular data rate, resulting in correct ML model training. The transmission power of the Base Station (BS) is maintained at a consistent level, which is set below a certain limit. The activation of a given number of RIS elements is determined based on the signals received from the Multiple-Input Multiple-Output (MIMO) antennas. An RIS element is selected for each signal based on the highest received power among all subcarriers. The task above involves the computation of the ω matrix to enhance operational efficiency and minimize the system's overall power consumption.

The restricted availability of channel status information at the Base Station hinders the practicality of directly computing the optimization function. In real-world situations, users must convey their input on the received data rate, while the Base Station knows its own transmit power. Furthermore, a thorough evaluation is conducted to analyze the impact of individual values on the system's overall communication and energy efficiency while considering the RIS components' phase shift and ON/OFF state. The objective function can be seen as a function characterized by a black box representation. Note that the worst-case scenario can be taken the scenario without the RIS system. The problem space exhibits discontinuous and non-smooth properties, and analytical computation for optimization is unfeasible. The current difficulty might be framed as the task of forecasting sequential data.

Deep learning algorithms can discover subtle relationships between input and output variables. In the context of this framework, the input variables consist of the signal characteristics (shown in Section IV-B1) related to the communication achieved between the BS and the RIS, the positions of the subcarriers in the signal, the settings of the individual RIS elements, and the transmission power. The output variable is linked to the optimal signal quality that can be achieved by the RIS, by restricting data rate to achieve maximum energy efficiency.

During the training phase, the base station (BS) utilizes the RIS to facilitate data transmission to the users. Subsequently, the users participate in computational procedures to determine the objective value and provide input to the BS. The Mean Squared Error (MSE) is computed by the Base Station (BS) to quantify the discrepancy between the observed outcome and the intended outcome. Following this computation, the revised configuration is communicated to the controller of the Remote Intelligent System. Ultimately, the reduction of the MSE is achieved by the utilization of the training samples.

The optimization landscape is challenging due to its non-smooth and discontinuous nature. Traditional analytical methods are often inadequate for such complexities. A contemporary solution views this optimization as sequential data prediction. Feedback DNN, Long Short-Term Memory (LSTM) networks, and ML approaches in general shine in this paradigm, capturing intricate temporal dependencies and discerning nuanced system parameter relationships. Employing ML allows for understanding various data facets, from transmission power to RIS configurations. The RIS controller undergoes periodic ML-guided updates, with the MSE metric validating the accuracy across training instances. Thus, we aim to identify the correct ω matrix based on the prediction of the reflected signal parameters and by having a predefined SNR or data rate.

IV. METHODOLOGY

A. METHODOLOGY DETAILS AND THE ROLE OF REFLECTIVE INTELLIGENT SURFACE (RIS) IN OUR APPROACH

The overarching goal of our methodology is to maximize energy conservation in wireless communication systems without compromising the efficiency of the communication process. Achieving this objective entails navigating a non-linear problem space, which is aptly approached using Deep Learning techniques. Here, we delve deeper into the methodology and highlight the pivotal role of the RIS in this context. This dual-objective optimization challenge inherently possesses non-linearity. The proposed methodology uses deep learning predictions so that the BS and RIS dynamically tweak its configurations. Accuracy assessment is done via the computation of the MSE between the model's predictions and actual observations, while the aim is to minimize this error across varied training instances. For the Antenna configuration, the setup utilizes antennas equivalent in number to the *"Total Used Subcarriers"* that OFDM (Orthogonal Frequency-Division Multiplexing) can support. RIS also actively modulates the wireless signal environment, allowing software-controllable wireless communication. Key aspects of RIS in our methodology include:

- **Signal Reflection and Modulation**: RIS's primary function is to relay signals to users by adjusting the phase shifts across its elements, encapsulated in the ω array.
- **Energy Conservation**: RIS, by directing signals appropriately, optimizes energy usage in wireless transmissions. It focuses on constructive interference at the intended user's location, minimizing energy wastage.
- **Channel State Information (CSI) Influence**: The CSI between the RIS and users, denoted by F, is of paramount importance. RIS actively shapes this CSI, significantly influencing system performance.
- **Deep Learning Predictions**: Our methodology harnesses deep learning to predict RIS's optimal signal relay characteristics. These predictions rely on the "HLS Structure," the input signal received by RIS. The goal is to predict the best reflection properties, particularly the best ω array, ensuring optimal received signals.
- **Dynamic Adjustability**: RIS's dynamic reflection property adjustment, influenced by deep learning model predictions, ensures optimal communication conditions, further guided by the Base Station (BS).

In conclusion, the RIS emerges as a keystone in our methodology. It not only provides a dynamic and adaptive medium but also, in conjunction with ML, revolutionizes wireless communication efficiency and energy optimization.

B. ML TRAINING

1) ML FEATURE VECTOR

The feature vector x, which is acting as the input feature in our investigation, comprises:

- Signal characteristics (i.e., signal power, interference, amplitude, and phase components).
- Indices ppositions: The indices ('ppositions') represent an array of indices used to select specific subcarriers from scheme_Channels_Structure for calculations, storing real and imaginary parts, and representing subcarriers of interest or reference subcarriers within the simulation. The ppositions are used to extract real and imaginary parts of channels from the scheme_Channels_Structure data structure.

The formulated target vector y, which is also acting as the input feature in our investigation, encapsulates:

- The apex signal characteristics aligned with the required SNR.
- Ancillary parameters such as mobility (with a bias towards high mobility), the channel model (VTV), modulation order (SDWW_QPSK), and the adopted scheme (DPA_TA).
- Indices dpositions: The indices ('dpositions') represent the actual or ground-truth channel values or features. The dpossitions represent the positions of the data subcarriers within the set of all active subcarriers (denoted by Kset in the code) that are used by the signal. The dpositions are used to extract real and imaginary parts of channels from the True_Channels_Structure data structure.

The output feature from our ML model will be a unique dposition index.

2) UNDERSTANDING THE ROLE OF INPUT AND OUTPUT FEATURES FOR NEURAL NETWORK TRAINING

In the realm of wireless communications, the matrices **Dataset_X** and **Dataset_Y** play pivotal roles as input and output features, respectively, for training a series of neural network models: LSTM, BLSTM, RNN_BLSTM, RNN, and FeedbackDNN. Here's a comprehensive elucidation:

a: DATASET_X: THE INPUT FEATURES MATRIX

- *Dimensions and Significance*: **Dataset_X** is a three-dimensional matrix representing the input features. Its dimensions span the number of subcarriers (*nSC_In*), symbols (*nSym*), and the entire dataset size. These features provide insights into the evolving nature of wireless channels over specific time intervals.
- *Handling Complex Data*: Recognizing the complex essence of wireless data, **Dataset_X** captures both the real and imaginary components of the channel, enriching the input feature set for models like LSTM and FeedbackDNN.
- *Integration of Multiple Data Sources*: This matrix effectively fuses data from varied sources, such as the *HLS_Structure* and the *scheme_Channels_Structure*, ensuring the ML models receive a holistic view of the input scenario.

b: DATASET_Y: THE OUTPUT FEATURES MATRIX

- *Dimensions and Role*: **Dataset_Y**, also three-dimensional, embodies the output features that the neural networks strive to predict.
- *Real-World Scenario Representation*: Populated by genuine channel data from the *True_Channels_Structure*, this matrix is the gold standard, allowing ML models to measure and optimize their predictive prowess.
- *Complex Data Segregation*: Echoing its counterpart, **Dataset_Y** splits data into real and imaginary components, providing a full-fledged output feature set for comparison and learning.

For additional details regarding the datasets utilized and the parameters/features of the dataset, please refer to the Appendix at A-B.

c: SYMBIOTIC PURPOSE FOR MODEL TRAINING

The synergy between **Dataset_X** as the input features and **Dataset_Y** as the output features is pivotal. Together, they form the crux of the training regimen for models such as LSTM, BLSTM, RNN_BLSTM, RNN, and FeedbackDNN. By consistently feeding **Dataset_X**, **Dataset_Y** into these models and calibrating their predictions against the unique selection of dposition of the investigated subcarrier, these neural networks are trained to yield optimized performance in real-world wireless communication scenarios.

For more information about the Terms regarding the **Dataset_X**, **Dataset_Y** and explanation about them along with the definition set and used in the provided code, it can be found in Appendix Section A.

d: INVESTIGATING THE SELECTION OF THE GENERATED DATASET

Addressing the relevance of the dataset generated for our study, compared to other existing datasets in the literature, necessitates a comprehensive analysis of its characteristics, such as diversity, scale, realism, and applicability to real-world scenarios. The datasets utilized in ML for RIS beam management are pivotal for developing, testing, and validating algorithms. Our dataset was meticulously curated to fill the gaps identified in existing datasets, specifically tailored to test and validate the efficacy of our proposed ML techniques for RIS beam management. It offers a unique combination of attributes tailored to the challenges of optimizing RIS-assisted communications, including scenarios with high mobility for testing algorithms in dynamic environments, a variety of environmental conditions to simulate realistic settings, diverse RIS configurations for extensive scalability and adaptability testing, and detailed Channel State Information (CSI) for the development and testing of algorithms that utilize deep insights into channel conditions for optimized beam management.

To further elaborate on the creation and relevance of our dataset, we examined the OFDM parameters as outlined in the IEEE 802.11p standard, generating a dataset that covers a broader range of scenarios than those available in existing datasets. This approach enabled us to thoroughly investigate high and low mobility scenarios and assess various encoding modes' outcomes, alongside optimizing transmission strategies directly from the Base Station (BS) to the User Equipment (UE) and via RIS to the same UE. This detailed methodology in dataset generation, inspired and informed by existing data collections such as those by Rossanese et al. [35] and Tewes et al. [36], has allowed us to develop a dataset that not only addresses existing gaps but also introduces new dimensions for RIS research, particularly in the complexities of varying mobility scenarios and encoding schemes.

3) THE INVESTIGATED ML MODEL DESIGNS

The `LSTM` model, designed with a single `nn.LSTMCell`, manages long-term dependencies by initializing with a specific input size and LSTM size, processing data through the cell to generate an output of size 96; it captures general data trends but might miss rapid changes. The `BLSTM` model, augmenting the LSTM with a bidirectional layer (`nn.LSTM`), doubles the LSTM output due to bidirectionality and then maps it to size 96, capturing both forward and backward data sequences but possibly introducing slight delays. The `RNN` model integrates an `nn.RNNCell` to identify temporal patterns; after initializing with an input and RNN size, data streams through the cell, outputting size 96, and while it's adept at capturing actual values, there's an overfitting risk. The `RNN_BLSTM` combines an `nn.RNN` and a bidirectional `nn.LSTM`; data first traverses the RNN layer, then the bidirectional LSTM, making it adept at matching actual values, albeit occasionally underestimating amplitudes. Lastly, the `FeedbackDNN` is structured around feed-forward layers and feedback loops; built with a sequence of linear and ReLU layers, a feedback mechanism projects data back to the input dimension, and after iterative feedbacks, a final linear layer yields the output; while capturing the overall data trend, regularization might be necessary to curb overfitting.

4) DEEP LEARNING OPTIMIZATION

Considering the discontinuities and complexity of the problem, traditional analytical optimization could be more feasible. Instead, a sequential data prediction model leveraging Deep Learning is suggested. Specifically, using ML networks can unravel the intricate relationships between inputs and outputs. It can be trained for energy conservation by feeding the model with parameters like transmission power, spatial dynamics between user devices and the RIS, and RIS configurations. This configuration, refined via the Mean Squared Error between predicted and actual results, demonstrates the future of sustainable, intelligent wireless communication systems, synergizing systems integration, intelligent surfaces, and deep learning.

TABLE 2. ML model configurations and hyperparameters.

Model	Hyperparameters	Layers Description
LSTM	Input Size: 104, LSTM Size: 5	`LSTMCell(input_size, lstm_size), Linear(lstm_size, 96)`
BLSTM	Input Size: 104, LSTM Size: 5	`LSTM(input_size, lstm_size, bidirectional=True), Linear(lstm_size * 2, 96)`
RNN_BLSTM	Input Size: 104, RNN Size: 2, LSTM Size: 5	`RNN(input_size, rnn_size), LSTM(rnn_size, lstm_size, bidirectional=True), Linear(lstm_size * 2, 96)`
RNN	Input Size: 104, RNN Size: 5	`RNNCell(input_size, rnn_size), Linear(rnn_size, 96)`
FeedbackDNN	Input Size: Variable, Hidden Sizes: [96], Output Size: 96, Feedback Loops: 2	`Feedback Linear(96, input_size), Final Linear(input_size, 96)`

C. ML MODELS DESIGN

Table 2 presents a detailed overview of configurations and layer descriptions for various ML models tailored for signal processing, including LSTM, BLSTM, RNN_BLSTM, RNN, and FeedbackDNN. For the LSTM and BLSTM models, an input size of 104 and an LSTM size of 5 are used, with the BLSTM also leveraging bidirectional processing to enhance its learning capacity. The RNN_BLSTM model incorporates an additional RNN layer with a size of 2 before its BLSTM layer, enabling a complex feature extraction from sequential data. In contrast, the RNN model simplifies this approach by using a single RNN layer with a size of 5, focusing on temporal dynamics with reduced complexity. The FeedbackDNN model stands out by not specifying a fixed input size and by incorporating feedback loops into its architecture, where it utilizes hidden sizes of 96 and includes two feedback loops to reintroduce outputs as inputs for enhancing the model's predictive capabilities. This table succinctly encapsulates the structural components and hyperparameter choices that differentiate these models, highlighting their specialized architectures designed for optimizing signal processing tasks.

D. INVESTIGATION ON TEST AND TRAINING PERCENTAGE OF DATA USING K-FOLD CROSS-VALIDATION

In our investigation into the optimal division of data for training and testing purposes, we employed the method of k-fold cross-validation to ensure the robustness and generalizability of our ML models tailored for RIS beam management. The k-fold cross-validation technique, detailed in Algorithm 1, systematically divides the dataset into 'k' distinct subsets. It iteratively uses one subset for testing and the remainder for training, cycling through all subsets to comprehensively assess model performance. This method is highly regarded for its ability to provide a reliable estimation of model efficacy on unseen data by mitigating variance associated with random data splits. After thorough experimentation with varying 'k' values and assessing different training-testing splits using the k-fold cross-validation technique, we concluded that a 75-25 split of the data, where 75% of the data is used for training and the remaining 25% for testing, yields the most effective balance between model training and validation accuracy. This split, combined with the rigor of k-fold cross-validation, minimizes overfitting while ensuring substantial exposure to the training data, as articulated in the following algorithm:

Algorithm 1 K-Fold Cross-Validation

Require: Dataset D, Number of folds k, ML Model M
Ensure: Average model performance score
  Divide D into k equal subsets $D_1, D_2, \ldots, D_k$
  for $i = 1$ to k **do**
    $D_{\text{train}} = D - D_i$
    $D_{\text{test}} = D_i$
    Train model M on D_{train}
    Evaluate performance of M on D_{test}
    Record performance score P_i
  end for
  $P_{\text{avg}} = \frac{1}{k} \sum_{i=1}^{k} P_i$ **return** P_{avg}

This empirical investigation, as elucidated in the text and Algorithm 1, reinforces our selection of the 75-25 train-test split as the optimal choice for our study, ensuring a balanced approach to model training and evaluation.

E. THE PROPOSED ALGORITHM FOR GENERATION OF THE DATA AND PREPARATION OF THE DATA FROM MODEL TRAINING AND TESTING

Algorithm 2 focuses on utilizing RIS within the field of signal processing. The increasing significance of RIS in the realm of wireless communication can be attributed to its capacity to improve the quality of communication through intelligent reconfiguration of the propagation environment. The initial phase of the algorithm, fittingly termed Initialization, is all about building up the data groundwork. This study allocates a set of 1000 samples, and a standard 75-25 split is employed to distinguish between the training and testing data. The element of uniqueness arises from the random selection of training indices (ppositions/dpositions), introducing a degree of randomness to the training set with each iteration of the algorithm. The testing samples are inherently comprised of the indices (ppositions/dpositions) that were not selected for training. To ensure the reproducibility of the data preparation process, the indices (ppositions/dpositions) are afterward stored in a .mat file. It is worth noting that the choice of this file format, which is commonly used for storing data

arrays, is influenced by using MATLAB® in this context. Upon further exploration, the subsequent part, entitled ''Generate Datasets for RIS Transmitted Signals,'' provides a pragmatic perspective on the procedure of simulating signal transmission inside an environment controlled by RIS.

The earliest stages encompass the establishment of diverse parameters, wherein individuals well-versed in the field of signal processing may identify terminologies such as Orthogonal Frequency Division Multiplexing (OFDM), modulation, and scrambler. Significantly, a channel model and other simulation parameters are developed, hence laying the foundation for the subsequent procedures. A mini-simulation is conducted for each signal-to-noise ratio, denoted as EbN0dB. The simulation involves the transmission and reception of signals, followed by channel estimation using the IEEE 802.11p LS Estimate. This estimation method is designed exclusively for vehicle communications and utilizes a least squares estimate. This section culminates in the process of deciphering the signals that have been received, as well as documenting any errors and metrics. These elements are of utmost importance in assessing the system's overall effectiveness. As mentioned above, the findings are recorded following the utilization of particular settings, leading to the computation of metrics such as bit error rate (BER) and normalized mean square error (NMSE) (shown in Section V-E). The metrics mentioned above hold significant recognition within the field of signal processing, particularly in system performance assessment, with a specific emphasis on communication systems. The final segment of the methodology, titled ''Preparing Datasets for ML,'' acknowledges the increasing tendency to combine ML methods with signal processing to improve overall performance. This section pertains to the curation of data in a manner that is appropriate for utilization in ML models. The indices (ppositions/dpositions) corresponding to the training and testing data that were previously designated are retrieved. The method generates comprehensive data for both settings. Every configuration requires the specification of particular parameters, and for each EbN0dB value, previous simulation outcomes are utilized. The subsequent stages are when the complexity of signal processing becomes evident.

Two datasets have been prepared, namely Dataset_X (representing the input) and Dataset_Y (representing the selection of results); note one of the dposition will be selected as the best signal characteristics as output. The input data consists of the real and imaginary components of a structure referred to as HLS_Structure, which is augmented with the RHP (Right Half Plane) and IHP (Imaginary Half Plane) values. This particular configuration potentially serves as preambles or sequences that aid in the process of signal detection or synchronization. The dimensions of this dataset are subsequently rearranged to ensure compatibility or optimize performance. Similarly, the output dataset is derived from the True_Channels_Structure, representing accurate and factual channel features. The dataset is also subjected to dimension permutation. Subsequently, both datasets are preserved with the prospective purpose of utilizing them for training a machine-learning model later in time. Finally, the supplementary information supplied in Appendix Section A-B, such as True_Channels_Structure, HLS_Structure, and DPA_TA_Structure, provide insights into the specific data structures that the algorithm handles. These entities appear to correspondingly retain channel attributes, preamble information, and time alignment details. Each of these factors offers distinct perspectives: the accurate transmission channel information, the particular sort of preamble employed in the system, and information regarding time alignment, which is of utmost importance in situations involving multi-path or multi-antenna setups to guarantee synchronization.

Algorithm 2 provides a comprehensive framework for approaching RIS-based signal processing, encompassing several stages such as setup, simulation, and dataset preparation specifically designed for ML applications. The use of ML exemplifies the progression of traditional signal processing methods as they adapt to contemporary computer approaches.

Note that Appendix Section A-C provides a more symbolic implementation of the proposed algorithm shown in Algorithm 2.

F. THE PROPOSED ALGORITHM FOR REFLECTING ANGLES CALCULATION BY RIS

The foundation of Algorithm 3 is grounded on data obtained from a structure known as ''True_Channels_Structure'', which is provided by the Base Station (BS). The data from this structure comprise the beams that the Reflecting Intelligent Surface (RIS) will manage and direct toward the User Equipment (UE). Following the retrieval of this data, the output dataset, labeled Y, is computed simulations for all possibilities of the dposition signal characteristics. Note that the dposition index will be calculated using a Feedback Deep Neural Network (DNN). This DNN plays a pivotal role in ensuring that the optimized signal's prediction is accurate and efficient. Once Y is determined, the algorithm begins calculating a specific value denoted by r. This calculation is governed by a formula integrating multiple parameters, with the reflection angle symbolized as ω, being of particular significance. By leveraging the equation mentioned above, the algorithm precisely computes the value of ω that is conducive to achieving the stipulated data rate and optimal power consumption. Post this calculation, the algorithm employs the advanced capabilities of MIMO (Multiple-Input, Multiple-Output) antennas. The primary function of these antennas within the algorithm is to accurately align all indices or dispositions in the direction of the computed angle, ω.

The culmination of the algorithmic process sees the RIS aligning the signal angle. This action ensures that the beams, originating from the True_Channels_Structure, are appropriately reflected towards the User Equipment (UE). The algorithm's efficacy is validated by whether the reflections lead to attaining the desired target. If this target is met, the algorithm successfully outputs the optimized signal and the reflection angle ω based on the dposition index selected. If not,

Algorithm 2 RIS-Based Signal Processing Approach

procedure RISApproach
  Initialization:
  Set total samples to 1000.
  Designate 75% of samples for training and 25% for testing.
  Randomly select training indices (ppositions/dpositions).
  Identify the remaining indices (ppositions/dpositions) as testing samples.
  Save both training and testing indices (ppositions/dpositions) to a '.mat' file.
  Generate Datasets for RIS Transmitted Signals:
  Define OFDM, modulation, scrambler, coder, interleaver, channel model, and simulation parameters.
  for each value of EbN0dB **do**
    Simulate transmission and reception of signals.
    Channel estimation using IEEE 802.11p LS Estimate.
    Decode received bits.
    Store errors and other metrics.
  end for
  Save results based on configuration.
  Compute BER and NMSE metrics.
  Save final simulation parameters.
  Prepare Datasets for ML:
  Load testing and training data indices (ppositions/dpositions).
  for configuration in {'training', 'testing'} **do**
    Set current loop configuration.
    Define simulation parameters.
    for each value of EbN0dB **do**
      Load simulation results.
      Prepare Input Dataset (Dataset_X):
      Extract real and imaginary parts of HLS_Structure.
      Append RHP and IHP to Dataset_X.
      Permute the dimensions of Dataset_X.
      Prepare Output Dataset (Dataset_Y):
      Extract real and imaginary parts of True_Channels_Structure.
      Append data to Dataset_Y.
      Permute the dimensions of Dataset_Y.
      Save datasets.
    end for
  end for
end procedure

a notification is triggered, indicating the non-achievement of the target. In essence, this algorithm seamlessly integrates the data from the True_Channels_Structure, the predictive prowess of the Feedback DNN, reflection angle calculations, and the functionalities of MIMO antennas and RIS to ensure the delivery of optimized signals to the UE.

Algorithm 3 Optimized Signal Prediction and Reflection Angle Calculation

Require: True_Channels_Structure given from BS
Ensure: Optimized signal and correct reflection angle
procedure OptimizeSignal(True_Channels_Structure)
  $\mathbf{Y} \leftarrow$ Extract output data from True_Channels_Structure given from BS
  Predict optimized signal based on $\mathbf{Y}$
  $\mathbf{r} \leftarrow \mathbf{F} \times \omega \times \mathbf{A} \times \mathbf{W} \times \mathbf{s} + \mathbf{u}$
  Calculate ω using eq. 24 for required Data Rate and power consumption from the disposition index selected and Dataset_Y
  Align all indices/dispositions towards ω using RIS
  Ensure RIS reflects beams correctly towards UE on RIS controller
end procedure

Figure 3 depicts the workflow of the ML process used in our methodology. The process begins with the "Start" node, signifying the initiation of the methodology. This leads to the first major phase, "Initialization," where the total samples are set to 1000, followed by the training-testing split, selection of training indices, setting aside testing samples, and saving the indices to a .mat file. After initialization, the process transitions to "Generate Datasets," where simulation parameters are defined, signals are simulated, channels are estimated, received bits are decoded and stored, and metrics like BER and NMSE are computed. Subsequently, the datasets are prepared for ML, which involves loading data indices, setting loop configurations, preparing input Dataset_X, and preparing output Dataset_Y. The final phase in the flowchart is "Optimize Signal & Reflection Angles," where the data extracted from the True Channels Structure is used to predict the optimized signal based on Y, calculate reflection angles (omega), align indices towards omega using RIS, and ensure the correct reflection towards the user equipment. The workflow concludes at the "End" node.

V. PERFORMANCE EVALUATION

This section provides the assumptions and terms used in the investigation, a comprehensive analysis of the configuration of the simulation environment, the evaluation metrics used in the examination, the validation of the models executed in terms of overfitting and underfitting with the use of k-fold investigation, and at the end the results.

A. ASSUMPTIONS, SIMULATION PARAMETERS AND CHARACTERISTICS

The investigation considers the assumptions shown in the following list, with the simulation parameters and characteristics shown in Table 3 and Table 4, respectively. Thus, we consider the following assumptions:

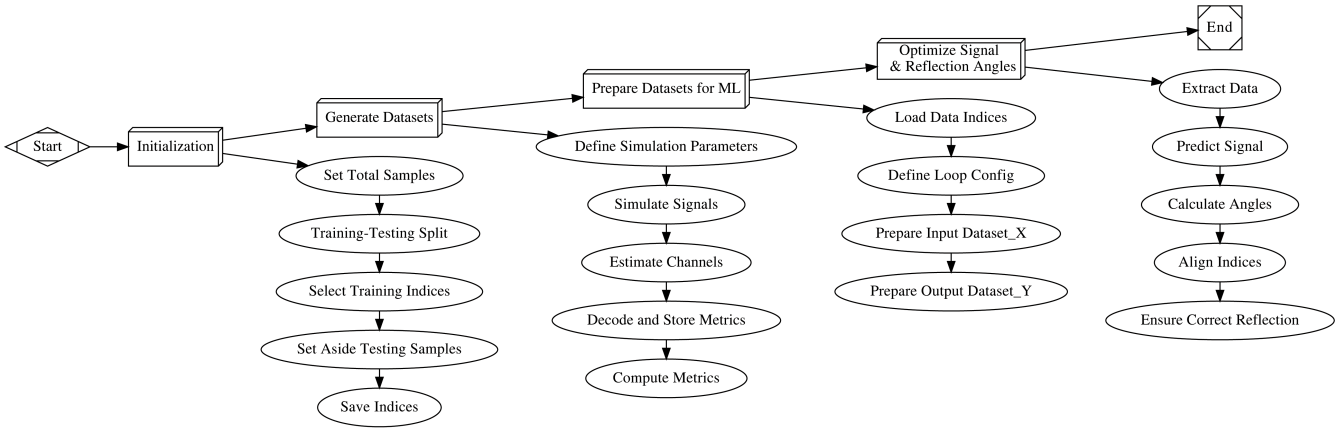

FIGURE 3. Flowchart depicting the ML process workflow in our methodology.

TABLE 3. Simulation parameters.

Parameter	Description
Noise Model Used	AWGN
Multiplexing	OFDM
Modulation Techniques	BPSK for binary data and various QAM variants (i.e., 'BPSK', 'QPSK' and '64QAM') otherwise
Data Randomization and Error Handling	scramInit = 93, convolutional coder
Interleaver	Used to combat burst errors
Channel Model for Vehicular?	'VTV_SDWW' model optimized for vehicular communications
Model Design and Deep Learning	Dropout layers, LSTM networks, RNN-BLSTM, RNN, BLSTM, Feedback DNN networks
Input and Output Features for Neural Network Training	Distinct Datasets
SNR Index	0 to 40 in steps of 5 dBs
Training Dataset Splitting	75% for training, 25% for validation
Mobility	High and low mobility
Channel Model	'VTV_SDWW' model
Training Scheme	'DPA_TA' scheme
Training SNR	40 dBs
Training Epochs	50
Batch Size	10
ML Size	5
Scheduler Step Size	10
Scheduler Gamma	0.8
Transmission Power per FB	20 W
Constant Data rate for RB	One Resource block(RB) have 12 sub-carriers (each carrier is 15 kHz)

TABLE 4. System characteristics.

Characteristic	Description
OFDM Bandwidth	10×10^6 Hz.
FFT Size	64.
Data Subcarriers	48.
Pilot Subcarriers	4
Zero Subcarriers	12
OFDM Symbols per Frame	20 .
Guard Interval	1.6 μs
Data Scrambling	Achieved with scramInit = 93 per the IEEE 802.11p standard.
Convolutional Coder	Used for error detection and correction with a constraint length of 7.
Interleaving	Used to combat burst errors with a matrix structure having 16 rows.
Performance Metrics	SNR, Eb/N0, NMSE, BER
Dropout Layer	Prevents overfitting with a rate of 0.2.
Deep learning architectures use	LSTM, BLSTM, RNN_BLSTM, RNN, FeedbackDNN.
Dataset_X and Dataset_Y	Input and output matrices for neural network training.

1) The study assumes that the Reconfigurable Intelligent Surfaces (RISs) used in the wireless communication system are properly configured and functional, without hardware or deployment issues that could affect their performance.
2) It is assumed that the RISs are equipped with the necessary sensors and actuators to adjust their reflecting elements accurately in response to control signals, allowing for effective beamforming and beam steering.
3) The investigation assumes that the wireless communication environment does not include substantial external interference sources that could significantly impact the performance of the RIS-based system.
4) It is assumed that the RISs and user equipment (UE) have stable power supplies and do not suffer from power fluctuations that could disrupt communication.
5) The study assumes that the Feedback DNN and other ML approaches for channel estimation are correctly implemented and trained with representative data, resulting in accurate channel estimates.
6) It is assumed that the wireless communication channels between RISs and UEs remain relatively stable during the time of data collection and evaluation without rapid and unpredictable variations.
7) The investigation does not address the impact of multiuser interference in the considered scenarios, focusing primarily on the performance of individual communication links between RISs and UEs.
8) We assume a communication system that utilizes RIS elements for beamforming and communication.
9) The energy harvested is calculated for a 1-second duration with a transmission of 1000 bits.

B. SIMULATION ENVIRONMENT

Parameters defined in the "IEEE 802.11p Spec" standard were used in the simulation environment. With the aid of MATLAB® and its 5G toolkit, a brute-force simulation approach is instituted. For specified SNR values and other parameters, the simulation pinpoints the optimal signal characteristics for individual locations, termed as the *"true channels structure"*. Implicitly, these determinations correspond to specific configurations of the ω array. Moreover, it's imperative to grasp the foundational hardware context to comprehend the computational demands and functionality of the LSTM, BLSTM, RNN_BLSTM, RNN, and FeedbackDNN models. Let's consider a typical personal computer (PC) in use:

- **Processor**: Intel Core i7-10700K with 8 cores and 16 threads, clocked at 3.8 GHz.
- **Memory**: 32GB DDR4 RAM at 3200 MHz.
- **Storage**: 1TB NVMe SSD with up to 3,500 MB/s read and 3,300 MB/s write speed.
- **Graphics**: NVIDIA GeForce RTX 3070 with 8GB GDDR6 VRAM.
- **Operating System**: Windows 10 Pro 64-bit.

Such a system is capable of efficiently training and deploying neural network models. The processor offers high-speed computation, while the RAM ensures smooth multitasking and data processing—the rapid storage guarantees fast data access speeds, which is essential when training large dataset models. The GPU accelerates neural network computations and caters to demanding visual applications.

C. EVALUATION METRICS

1) TRAINING LOSSES

`train_losses` captures the disparity between the predictions made by the model and the actual outcomes during the training phase (as shown in Equation 29). It is the value of the cost function over the training dataset.

$$\text{Training Loss} = \frac{1}{N}\sum_{i=1}^{N} L(y_i, \hat{y}_i) \tag{29}$$

where L is a loss function (could be Mean Squared Error, Cross-Entropy, etc.), y_i is the actual value, $\hat{y}_i$ is the predicted value, and N is the number of training samples.

2) VALIDATION LOSSES

While `train_losses` is associated with the training dataset, `validation_losses` is the model's loss over the validation dataset (it is calculated similarly to the Equation 29). It effectively indicates overfitting: if a model's training loss keeps decreasing but its validation loss increases, the model is likely overfitting to the training data.

3) MEAN ABSOLUTE ERROR (MAE) LOSSES

`mae_losses` represents the average of absolute differences between predicted and actual observations (as shown in Equation 30). It provides a linear penalty for each unit of difference between the estimated and true values.

$$\text{MAE} = \frac{1}{N}\sum_{i=1}^{N} |y_i - \hat{y}_i| \tag{30}$$

4) MEAN SQUARED ERROR (MSE) LOSSES

`mse_losses` quantifies the average squared difference between the estimated values and actual values (as shown in Equation 31). It gives a quadratic penalty for errors.

$$\text{MSE} = \frac{1}{N}\sum_{i=1}^{N} (y_i - \hat{y}_i)^2 \tag{31}$$

5) ROOT MEAN SQUARED ERROR (RMSE) LOSSES

`rmse_losses` is the square root of the MSE (as shown in Equation 32). It provides the magnitude of the error in the same units as the output.

$$\text{RMSE} = \sqrt{\frac{1}{N}\sum_{i=1}^{N} (y_i - \hat{y}_i)^2} \tag{32}$$

6) R-SQUARED (R^2) VALUES

`r2_values` or the coefficient of determination is a statistical measure that explains the proportion of the variance in the dependent variable predicted from the independent variable(s) (as shown in Equation 33). It ranges from 0 to 1, with 1 being a perfect prediction.

$$r^2 = 1 - \frac{\sum (y_i - \hat{y}_i)^2}{\sum (y_i - \bar{y})^2} \tag{33}$$

where $\bar{y}$ is the mean of observed data.

7) ADJUSTED R-SQUARED (ADJ R^2) VALUES

`adj_r2_values` compensates for adding variables that don't improve the model (as shown in Equation 34). It adjusts based on the number of predictors in the model.

$$\text{adj\_}r^2 = 1 - \frac{(1 - r^2)(N - 1)}{N - k - 1} \tag{34}$$

where k is the number of predictors and N is the sample size.

8) AVERAGE PROCESSING TIMES

`avg_time`: captures the average time the ML model takes to process the input data, either during training or prediction. It offers a measure of the computational efficiency of the approach. This is usually computed in terms of milliseconds (ms) or seconds and is crucial for real-time applications where rapid decision-making is essential. With these metrics at hand, we can ascertain not only the accuracy and efficiency of our models but also diagnose and rectify potential issues such as overfitting or underfitting. They are a comprehensive toolkit to optimize and fine-tune our machine-learning approach.

9) FIGURE OF MERIT

To calculate the Figure of Merit (FOM) [37] using the provided metrics, we first need to define ''desired performance'' and ''undesired performance'' tailored to your specific application. Assume the following definitions:

- **Desired Performance:** Minimizing Training Loss, Validation Loss, MAE Loss, MSE Loss, RMSE Loss, and maximizing R^2 Value and Adjusted R^2 Value.
- **Undesired Performance:** Maximizing Average Processing Time.

The following is the definition of the desired and undesired performance metrics:

$$\text{Desired Performance} = \begin{pmatrix} \text{train\_losses} \times \\ \text{validation\_losses} \times \\ \text{mae\_losses} \times \\ \text{mse\_losses} \times \\ \text{rmse\_losses} \times \\ \text{r}_2\text{\_values} \times \\ \text{adj\_r}_2\text{\_values} \end{pmatrix}^{-1}$$

$$\text{Undesired Performance} = \text{avg\_time}$$

Using these assumptions, we construct the FOM formula as:

$$FOM = \frac{\text{Desired Performance}}{\text{Undesired Performance}}$$

D. UTILIZATION OF THE K-FOLD VALIDATION FOR OVERFITTING/UNDERFITTING AVOIDANCE

Balancing bias and variance in ML is crucial for a model's performance on unseen data. Overfitting occurs when a model becomes too attuned to the training data, capturing its noise and random fluctuations. As a result, an overfitted model, despite performing well on the training set, often struggles with new data due to its high variance and low bias [38]. On the other hand, underfitting arises when a model fails to grasp the training data's underlying patterns. This lack of complexity results in a model with high bias and low variance, leading to suboptimal performance on both the training and new data [38]. One effective approach to combat both overfitting and underfitting is employing K-fold cross-validation. In this technique, data is divided into k subsets. The model is then iteratively trained on $k - 1$ subsets and validated on the remaining one (as shown in the Section IV-D). This provides multiple angles of assessment and helps detect whether the model is overfitting (performing well on training but poorly on validation) or underfitting (poor performance on both training and validation). By giving a holistic view of model performance across various data slices, K-fold cross-validation aids in fine-tuning models for a more balanced bias-variance trade-off [38].

E. SIMULATION RESULTS AND ML APPROACHES COMPARISON

This section comprehensively analyzes several advanced ML techniques and approaches utilized in high-mobility scenarios. With the system model presented in Section II, the optimization problem formulated for the proposed work can only be evaluated with real-life network conditions. The LSTM, BLSTM, RNN_BLSTM, RNN, and FeedbackDNN schemes here recursively process beam sequences at every time step of the input. These ML approaches are considered advanced, using neural networks and their various adaptations. Our examination is the prediction of the maximum signal that the BS and RIS can achieve. Next, we compare the performance of each ML approach. Finally, we show how the RIS performance improved regarding power efficiency using the Feedback DNN, the best-selected ML approach based on the executed comparison.

a: LSTM (LONG SHORT-TERM MEMORY)

LSTMs are explicitly designed to circumvent the long-term dependency issue. Their ability to remember information for prolonged periods makes them particularly apt for high-mobility scenarios where the context and signal structure could vary over extended intervals. Figures 4a and 4b present a detailed analysis of the performance of the LSTM model. They encompass various aspects, including the comparison between expected and actual results, as well as the training dynamics of the model during 50 epochs.

Figure 4a offers a concise overview of the LSTM model's predictive capabilities. In general, the model has a satisfactory level of accuracy in capturing the trend and dynamics observed in the actual data. Although the projected values do not exhibit full alignment with the actual values in every instance, they roughly adhere to the overall trend. The model exhibits a minor delay in areas characterized by significant slopes, potentially suggesting difficulty capturing fast fluctuations. Nevertheless, the regularity in adhering to the overall pattern indicates that the LSTM model provides a reliable predictive framework for this specific dataset.

Figure 4b illustrates the progression of loss metrics for the training and validation datasets. The training and validation loss both demonstrate a rapid decrease in the early epochs, indicating a prompt adaptation of the model's parameters. Following the initial significant decline, it can be observed that the validation loss begins to stabilize around the 20^{th} until 30^{th} epoch. This observation perhaps suggests that the model can effectively generalize to unfamiliar data.

In summary, the model demonstrates strong predictive capabilities, and the training observations underscore the significance of being cautious about overfitting, particularly during the later phases of the training procedure.

b: BLSTM (BIDIRECTIONAL LONG SHORT-TERM MEMORY)

An extension of the LSTM, the BLSTM processes data from past to future and vice versa, offering a two-way

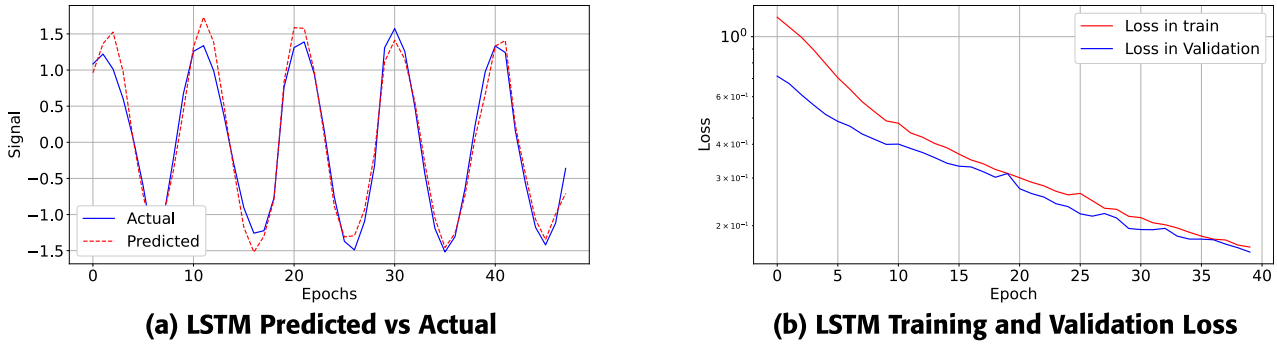

(a) LSTM Predicted vs Actual (b) LSTM Training and Validation Loss

FIGURE 4. LSTM performance evaluation.

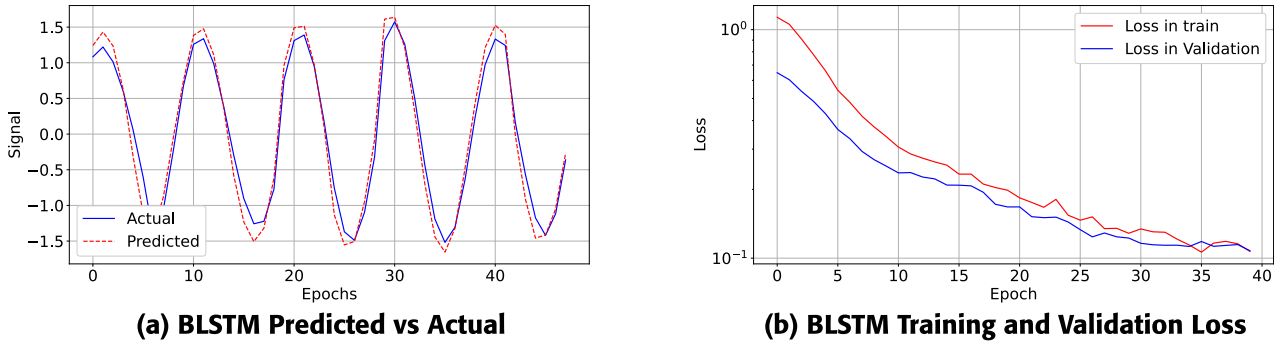

(a) BLSTM Predicted vs Actual (b) BLSTM Training and Validation Loss

FIGURE 5. BLSTM performance evaluation.

information passage. This bidirectionality ensures a holistic understanding of the input data, capturing patterns that might be overlooked in a unidirectional approach.

Figure 5a compares the forecasted values derived from a Bidirectional Long Short-Term Memory (BLSTM) model and the observed values. The x-axis appears to depict discrete time intervals or individual data points, while the y-axis exhibits a range of values spanning from -0.6 to 0.4. The projected values strongly correlate with the observed values in numerous geographical areas, particularly near the highest and lowest points, suggesting that the model has successfully captured some inherent patterns. Nevertheless, certain regions, particularly near the more pronounced peaks and troughs, exhibit a tiny temporal discrepancy between the projected and observed curves. This implies that although the model can forecast overall patterns, it may exhibit a minor delay in its ability to react to sudden shifts. There are slight disparities between the projected and observed values. However, they do not appear to be very substantial.

Figure 5b illustrates the progression of training and validation loss for the BLSTM model throughout numerous epochs. The observed trend in the lowering values of both the training and validation loss across successive epochs suggests that the model is progressively acquiring knowledge and enhancing its performance. During the early stages of the experiment, the training and validation losses exhibited a similar magnitude. However, a discernible disparity emerges between the two curves about the 35^{th} epoch. The pace of decrease in the training loss surpasses that of the validation loss. The observed divergence indicates the possibility of overfitting, wherein the model may excessively adapt to the training data and hence lose its capacity to generalize well on unknown validation data. In the later stages of the epochs, particularly after the 40^{th} epoch, evidence suggests that the validation loss exhibits a decline that is more comparable to the training loss. This observation implies the occurrence of a late-stage stabilization or convergence. The BLSTM model exhibits notable efficacy in its learning capabilities, particularly during the early epochs.

In terms of prediction, although the model has a satisfactory ability to capture the overall pattern of the data, there is potential for improvement through fine-tuning or incorporating supplementary characteristics to mitigate the modest delay in response to sudden fluctuations.

c: RNN (RECURRENT NEURAL NETWORK)

Fundamentally designed to recognize patterns across time intervals, RNNs excel at processing data sequences. Their iterative loop mechanisms allow them to maintain and update their states over time, making them a natural choice for time-varying scenarios like high-mobility communication environments.

The predictions of the recurrent neural network (RNN), closely approximate the actual values in Figure 6a. This implies that the model has attained a satisfactory degree of precision in its prognostications. The graph has distinct

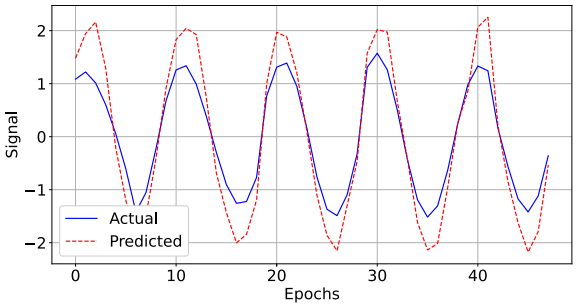

(a) RNN Predicted vs Actual

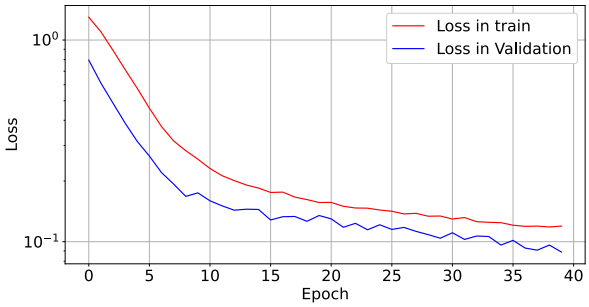

(b) RNN Training and Validation Loss

FIGURE 6. RNN performance evaluation.

zones, particularly near the 10^{th} and 30^{th} data points, where the projected values deviate from the observed values. These discrepancies may represent instances where the model encounters difficulties in accurately capturing the underlying patterns or instances where the data exhibits substantial fluctuations, which are the signal's peak values (from -1.1 to 1.5 and from $+1.1$ to 1.5).

Figure 6b depicts the progression of training and validation loss in an RNN model during a span of 50 epochs. The training and validation loss exhibit an initial high value, which decreases rapidly throughout the initial epochs. This observation suggests that the model is acquiring knowledge and enhancing its capabilities throughout the earliest stages of training. From around the 20^{th} epoch until the 40^{th} epoch, the validation loss demonstrates a tendency to reach a stable state, accompanied by a notable deceleration in the rate of decline. This observation suggests that the model may be approaching its maximum performance on the validation dataset. During training, it is routinely seen that the training loss remains smaller than the validation loss. There is a noticeable convergence between the training and validation loss lines. This implies that there is a convergence between the model's performance on the training data and its performance on the validation data. The graph's y-axis is logarithmically scaled, indicating that even minor apparent gaps correspond to substantial variations in loss values. This finding underscores the significant decrease observed during the early stages.

In summary, the recurrent neural network (RNN) model has a favorable learning pattern, as evidenced by the consistent decrease in both training and validation loss throughout the epochs. Nevertheless, it is imperative to exercise prudence and consider alternative measurements, examinations, and even supplementary validation or test sets to ascertain the model's resilience and prevent potential overfitting.

d: RNN_BLSTM (RECURRENT NEURAL NETWORK WITH BIDIRECTIONAL LONG SHORT-TERM MEMORY)

This model seamlessly fuses the RNN's inherent capacity to harness past information with the BLSTM's bidirectional prowess. Such a combination offers enriched temporal dynamics and improved learning capabilities.

Figure 7a shows that the RNN-BLSTM model exhibits a strong alignment with the actual values in multiple regions, indicating the satisfactory performance of the model; however, in the central region of the graph, the projected values tend to underestimate the amplitude of both the high and low points in comparison to the actual values.

Figure 7b demonstrates that both the training and validation losses consistently decline throughout the epochs, suggesting that the model is acquiring knowledge and enhancing its performance with increased exposure to data. The initial training loss exhibits a bigger magnitude yet exhibits a gradual and consistent decline across the epochs. This pattern suggests that the model is consistently optimizing its parameters and improving its ability to represent the training data accurately. As the epochs advance, in the vicinity of epochs 30-40, the loss experiences a slight uptick before resuming its downward trend. These tiny irregularities may suggest variations in the validation dataset or the model's challenges in effectively extrapolating to unfamiliar data points. As the number of epochs increases, the discrepancy between the training and validation losses diminishes, suggesting that the model is memorizing the training data and improving its ability to generalize to unfamiliar data.

The model has a notable learning trajectory during 50 epochs, steadily decreasing both training and validation losses.

e: FEEDBACKDNN (FEEDBACK DEEP NEURAL NETWORK)

Incorporating feedback mechanisms into DNNs, this approach accentuates the model's adaptability. FeedbackDNN can recalibrate based on the output's accuracy, ensuring enhanced robustness, particularly in dynamic environments where the signal's nature can alter rapidly.

Figure 8a demonstrates that this method can accurately depict the general pattern observed in the actual data.

In Figure 8b, we observe that both losses exhibit initial values that are relatively high.

Nevertheless, there is a noticeable decrease in the early stages, suggesting that the model rapidly acquired the ability to represent the data accurately. At approximately the 10^{th} epoch, there is a noticeable deceleration in the rate of

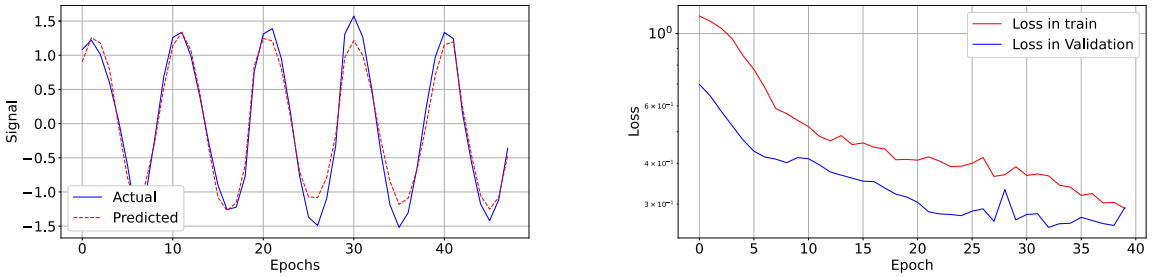

(a) RNN_BLSTM Predicted vs Actual

(b) RNN_BLSTM Training and Validation Loss

FIGURE 7. RNN_BLSTM performance evaluation.

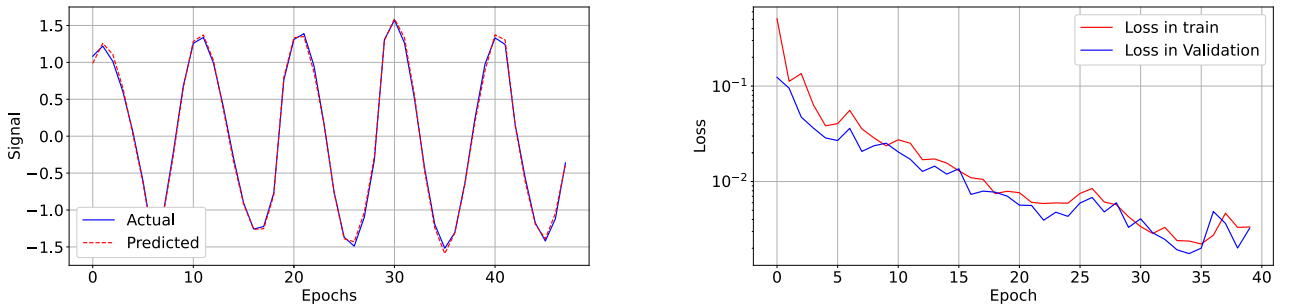

(a) FeedbackDNN Predicted vs Actual

(b) FeedbackDNN Training and Validation Loss

FIGURE 8. FeedbackDNN performance evaluation.

reduction, leading to a stabilization of both losses that implies that a significant portion of the learning process took place during the initial epochs, and the model may have begun to converge towards an ideal solution. Nevertheless, after the 10^{th} epoch, the validation loss displays oscillations, which means that its generalization performance on the validation data may not be consistently optimal. During subsequent epochs, particularly after the 40th epoch, it is observed that the validation loss occasionally exhibits an increase, while the training loss demonstrates a decrease or remains relatively stable. At the later stage of the training process, specifically around the 50th epoch, it can be observed that both the training and validation loss tend to reach a stable state.

In summary, it can be observed that the FeedbackDNN model demonstrates efficient learning during the early epochs. However, as the training process advances, indications of overfitting become apparent. Employing regularization techniques, implementing early stopping, or adjusting the design to attain a more optimal equilibrium between training and validation performance may be advantageous.

f: JOINT COMPARISON OF THE ML APPROACHES

In the relentless quest to optimize beam management within the increasingly intricate domain of wireless systems, especially those leveraging RISs, comprehensive evaluations of various techniques become invaluable. Table 5[1] is a testament to this exploration, outlining the performances of multiple methodologies against a suite of metrics pertinent to RIS's beam management optimization. The five different ML approaches presented earlier are summarised. Examining their Training and Validation Loss metrics provides insights into how well each model performs in learning from the training data and generalizing to unseen data. A lower loss indicates better performance. It appears that FeedbackDNN demonstrates superior performance by achieving the lowest documented losses. In contrast, the RNN_BLSTM model exhibited the largest training and validation losses, suggesting its relative underperformance in this regard. Upon examining the loss measures, namely Mean Absolute Error (MAE), Mean Squared Error (MSE), and Root Mean Squared Error (RMSE), it is evident that FeedbackDNN constantly exhibits superior performance compared to the other models. This is demonstrated by consistently achieving the lowest values across all three metrics. Once again, the RNN_BLSTM model demonstrates a tendency towards extreme values, resulting in the highest recorded values and hence exhibiting the lowest level of accuracy. Shifting our focus to the coefficient of determination, denoted as R^2 and $adjustedR^2$ values, FeedbackDNN demonstrates an almost impeccable alignment with the data, attaining the greatest values compared to all other models. On the other hand, the RNN_BLSTM model has the poorest fit, as indicated by its lowest values of R^2 and $adjustedR^2$. However, when considering computational efficiency, as measured by the average time metric, the RNN emerges as the most efficient model, exhibiting the shortest average time required to

[1]Note that Values for Train Loss, Validation Loss, MAE Loss, MSE Loss, RMSE Loss, R^2 Value, and Adjusted R^2 Value are unitless as they represent error metrics, coefficients, or ratios. Average Time is in milliseconds (ms).

TABLE 5. Performance metrics on beam prediction for RIS approaches, including figure of merit (FOM).

Model	Train Loss	Validation Loss	MAE Loss	MSE Loss	RMSE Loss	R^2 Value	Adjusted R^2 Value	Average Time (ms)	FOM Value
LSTM	0.1231	0.1074	0.2097	0.1074	0.2863	0.8891	0.8885	7.3659	0.0001
BLSTM	0.0875	0.0744	0.1779	0.0744	0.2384	0.9232	0.9228	22.5293	0.0000
RNN_BLSTM	0.2828	0.2659	0.3808	0.2659	0.4980	0.7256	0.7242	97.8453	0.0000
RNN	0.0933	0.0776	0.1822	0.0776	0.2468	0.9199	0.9195	4.6734	0.0010
FeedbackDNN	0.0130	0.0062	0.0474	0.0062	0.0661	0.9936	0.9935	10.0645	0.0042

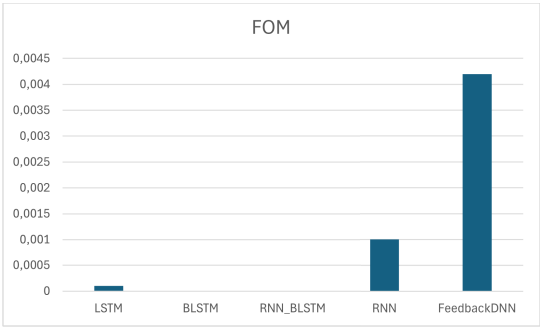

FIGURE 9. Figure of merit.

generate results. Interestingly, the RNN_BLSTM model, despite exhibiting subpar performance in the aforementioned measures, demonstrates the longest execution time, hence rendering it the least efficient. When comparing the performance metrics of LSTM and BLSTM models, it is observed that both models provide similar results, with BLSTM demonstrating a slight advantage. Nevertheless, it is important to acknowledge that BLSTM models require approximately three times more computational time than traditional LSTM models. This aspect should be considered, particularly when the application has strict time limitations.

In summary, while each method has its merits, the FeedbackDNN has superior accuracy and optimal alignment with the data distinctly surfaces as an optimal candidate for RIS beam management; it does not exhibit the highest speed among the models. Although RNN is known for its speed, it does not achieve the same level of accuracy as FeedbackDNN. The RNN_BLSTM model exhibits deficiencies in both its accuracy and speed. Hence, the selection of a model should involve a careful consideration of the trade-off between accuracy and time efficiency, taking into account the unique job requirements. This comprehensive evaluation underscores the pressing need for continued research in this domain. With beam management acting as a linchpin for efficient communication in systems like RISs, and given their burgeoning complexity, it's evident that a profound understanding and refinement of these methodologies can significantly uplift system throughput and reliability. The evolution in neural network-based techniques, such as LSTM and BLSTM, further accentuates the ongoing advancements in the field and the importance of staying abreast with the latest strategies. Moreover, the FOM values presented in Table 5 and Figure 9 provide a comparative insight into the performance of various models applied in beam prediction for RIS approaches. Notably, the FeedbackDNN model shows the highest FOM value of 0.0042, indicating a superior balance of prediction accuracy and computational efficiency among the models evaluated. In contrast, models such as RNN_BLSTM have the lowest FOM value (0.0000), which may be attributed to its significantly higher average processing time, as detailed in the table.

F. RIS PERFORMANCE IMPROVEMENT WITH THE FEEDBACK DNN

Figures 10 and 11 illustrate the BER performance of different modulation schemes (BPSK, QPSK, and 64QAM) in two scenarios: one with high mobility and one with low mobility. For each modulation scheme, the BER performance is plotted under 3 different conditions: (1) the case where a feedback mechanism controlled by a Deep Neural Network (DNN) is integrated, (2) the theoretical case that represents the calculated or optimal performance of the particular modulation, devoid of the obstacles encountered in practical situations and the case that incorporates a variant of "Dynamic Power Allocation" (named "DPA TA"). It is worth noting that the ideal cases in both modulations serve as benchmarks, representing the highest level that real-world modulation schemes strive to achieve. When comparing the performance of the Feedback DNN" and Dynamic Power Allocation schemes (DPA) for both modulations, it becomes apparent that the "Feedback DNN" schemes often exhibit a competitive advantage, particularly at lower E_b/N_0 values. This observation implies that integrating deep neural networks (DNNs) with feedback mechanisms has more resilience in situations involving high and low mobility compared to the strategies where DPA is used.

In the high-mobility scenario, 100 users are assumed to be moving around the wireless environment with speeds that vary between 14 m/s with 100 RIS elements, one for each user. Scenarios characterized by high mobility, such as the movement of vehicles or rapid fluctuations in the wireless environment, pose the difficulty of ensuring a continuous and reliable communication connection. Errors can be induced by phenomena such as fast fading, Doppler shifts, and developing interference patterns. The graph highlights the potential of employing advanced modulation schemes and approaches, such as deep neural network (DNN) feedback systems, to adapt to challenging conditions and improve overall performance effectively. Inspecting the results in

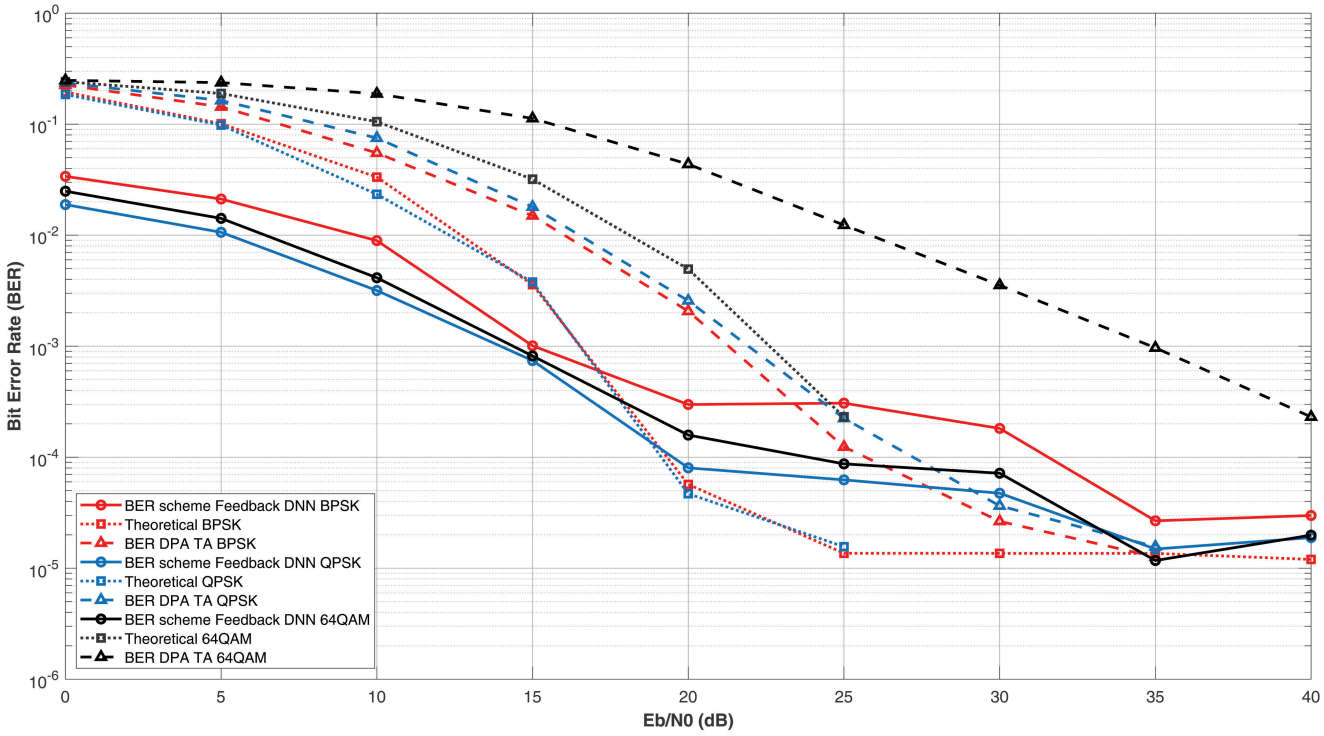

FIGURE 10. BER performance employing high mobility scenario.

Figure 10 it appears that the standout performer in terms of BER is the Feedback approach scheme for all modulation schemes. This approach not only seems to outperform the case where dynamic power allocation is used but also performs better than the theoretical (no RIS) case, especially at low E_b/N_0.

On the other hand, in the low mobility case, 100 users are assumed to be moving with speeds that vary between 1,4 m/s with 100 RIS elements, one for each user. Figure 11 demonstrates that much similar performance is achieved here with the Feedback DNN approach outperforming the DPA approach across the entire E_b/N_0 on both modulations. At the same time, it also has better performance than the theoretical case at low E_b/N_0 values.

The model's training loss is minimal, and very high accuracy has been achieved, as seen in the figures 8a and 8b. Thus, the Feedback DNN can be modeled in such a way as to have high convergence with minimal MSE, providing an overall improvement of beam management for channel estimation.

1) ENERGY HARVESTING ANALYSIS FOR FEEDBACK DNN 64QAM WITH RIS

In this subsection, we analyze the energy harvesting for the Feedback DNN 64QAM scheme with varying numbers of Reconfigurable Intelligent Surface (RIS) elements. The energy harvested is a crucial metric that indicates the system's ability to convert received signal power into usable energy for the device. The selection of RIS elements is made empirically by selecting the neighbouring RIS elements of the highest power beam received (note that they are selected squarely).

a: ENERGY HARVESTING CALCULATION

The energy harvested ($\mathbf{E}_{\text{harvested}}$) for a given scenario can be calculated using the following formula:

$$\mathbf{E}_{\text{harvested}} = \frac{\text{Total bits transmitted}}{\text{BER} \times \text{SNR}}$$

where:

- Total bits transmitted: 1000 bits (as per our assumption)
- BER: Bit Error Rate, already known
- SNR: Signal-to-Noise Ratio, calculated as $\frac{\mathbf{E_0}}{\mathbf{N_0}}$. We calculate the SNR for each scenario using the provided E0/N0 values. Then, we apply the formula to calculate the energy harvested for each scenario.

b: RESULTS ON MULTI TRANSMISSIONS AT RIS

The results of the energy harvesting analysis for Feedback DNN 64QAM with different numbers of RIS elements under both low-speed and high-speed conditions are summarized in Table 6.

Table 6 displays the energy harvested for Feedback DNN 64QAM communication systems with varying numbers of RIS elements under both low-speed and high-speed conditions. The results reveal a compelling trend in energy harvesting as the number of RIS elements increases. For

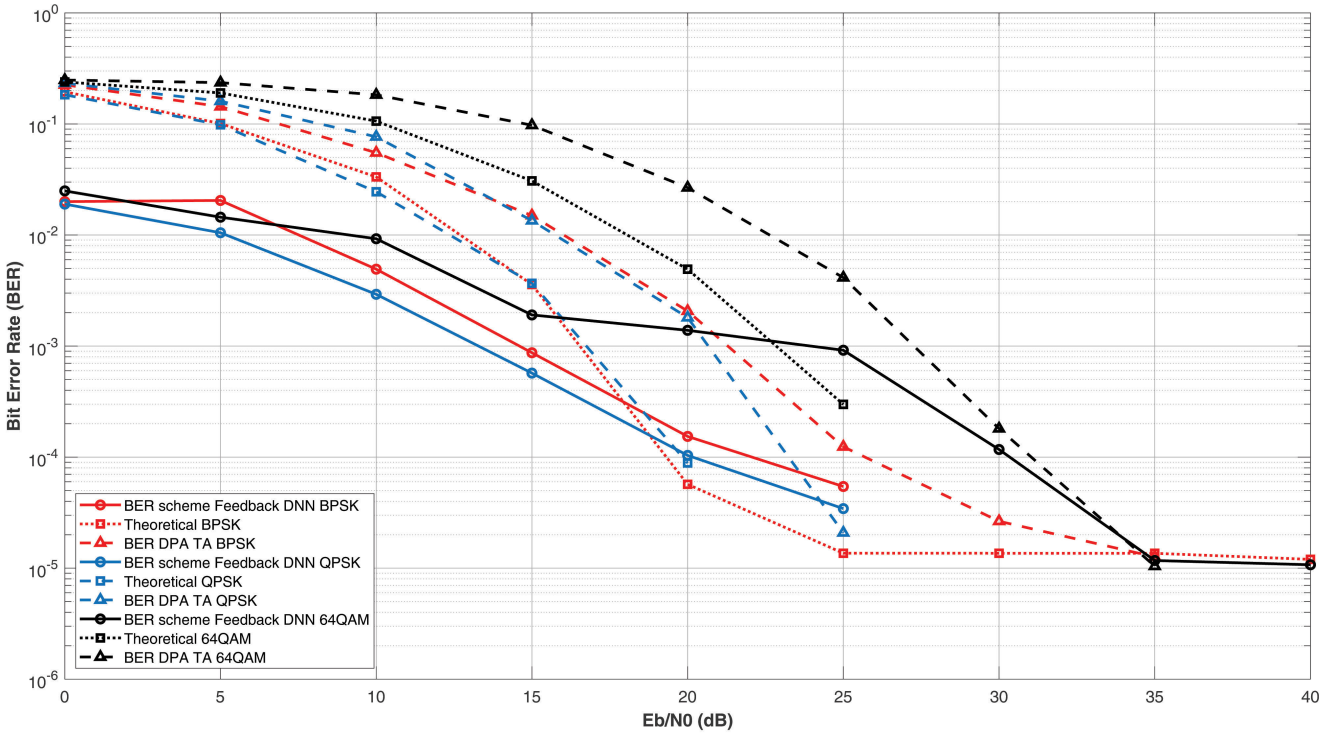

FIGURE 11. BER performance employing low mobility scenario.

TABLE 6. Energy harvested for feedback DNN 64QAM with different numbers of RIS elements.

RIS Elements	Energy Harvested (mJ) - Low Speed	Energy Harvested (mJ) - High Speed
5	40,048.06	25,785.24
10	69,070.31	38,734.69
20	108,038.03	57,848.58
50	524,109.01	115,914.92
80	721,500.72	173,208.84
100	1,090,512.54	206,614.77

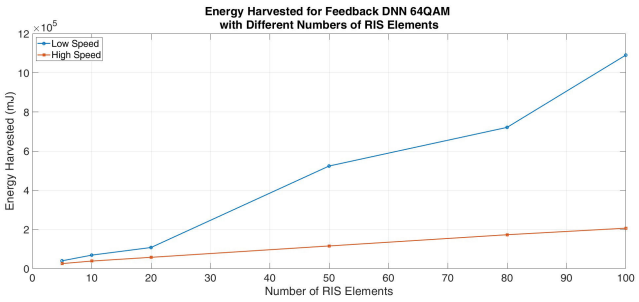

FIGURE 12. Energy harvested for feedback DNN 64QAM with different numbers of RIS elements.

the low-speed scenario, with only 5 and 10 RIS elements, the energy harvested is relatively modest, indicating limited energy accumulation. However, as the number of RIS elements grows to 20, there is a significant boost in the energy harvested, highlighting the positive impact of a larger RIS array. The trend continues, with 50, 80, and 100 RIS elements leading to substantial energy harvesting levels. This observation suggests that increasing the number of RIS elements can significantly enhance energy harvesting in Feedback DNN 64QAM communication systems when mobility is low. In the high-speed scenario, a similar trend is observed. Although the absolute values of energy harvested are lower than in the low-speed scenario, the relative improvement with a larger number of RIS elements is evident. This underscores the adaptability of RIS technology to enhance energy harvesting across varying mobility conditions. In conclusion, the results emphasize the potential benefits of utilizing a larger number of RIS elements for augmenting energy harvesting in Feedback DNN 64QAM communication systems, both in scenarios of low and high mobility. The energy harvested at different vehicle speeds when utilizing a Feedback DNN 64QAM communication scheme with varying numbers of RIS elements is depicted in Figure 12. It is evident from the graph that the amount of energy harvested increases significantly with the number of RIS elements. This trend is more pronounced at lower vehicle speeds. At higher speeds, while the increase remains consistent, the overall energy harvested is less than that at lower speeds. The analysis demonstrates the relationship between the number of RIS elements and the energy harvested. As the number of RIS elements increases, the energy harvested also increases significantly. This suggests that a larger number of RIS elements can improve the energy harvesting capabilities of the system, which can be valuable in wireless communication scenarios with energy-constrained devices. In summary, this

subsection provides insights into the energy harvesting potential of the Feedback DNN 64QAM scheme in RIS-enabled communication systems. The results highlight the importance of optimizing the number of RIS elements for enhanced energy harvesting in wireless communication.

c: RESULTS CONSIDERING A MULTI-USER SCENARIO

The results of the energy harvesting analysis for Feedback DNN 64QAM with different numbers of RIS elements under both low-speed and high-speed conditions, along with an investigation into the influence of the number of UEs, are summarized in Table 6. Note that the UEs are arranged in a grid-like pattern, with each UE positioned 50 meters from one another within each site at the same speed, according to the examination. This means that UEs are systematically spaced apart, forming a regular grid layout across the site.

TABLE 7. Energy harvested for feedback DNN 64QAM with different numbers of RIS elements and UEs.

RIS Elements	UEs	Energy Harvested (mJ) - Low Speed	Energy Harvested (mJ) - High Speed
5	5	40,048.06	25,785.24
10	10	69,070.31	38,734.69
20	20	108,038.03	57,848.58
50	50	524,109.01	115,914.92
80	80	721,500.72	173,208.84
100	100	1,090,512.54	206,614.77

The energy harvested for Feedback DNN 64QAM communication systems, as presented in Table 7, exhibits a notable trend influenced by the varying numbers of RIS elements and UEs. This trend reflects the system's responsiveness to increased RIS elements and UEs, indicating a substantial enhancement in energy harvesting. Specifically, the utilization of OFDM frequency bands contributes significantly to this phenomenon.

In low-mobility scenarios, where 5 and 10 RIS elements are employed, the energy harvested is relatively modest, particularly with fewer UEs. However, a noticeable increase is observed when the number of RIS elements and UEs is raised to 20, suggesting a positive correlation between the size of the RIS array, the number of UEs, and energy harvesting levels. This trend persists as the number of RIS elements increases to 50, 80, and 100, indicating substantial improvements, especially with more UEs. Similarly, the absolute energy harvested values in high-speed scenarios are lower than in low-speed scenarios due to the increased Doppler effect and faster fading rates experienced by the wireless signals. In high-speed scenarios, such as those encountered in vehicular communication, the rapid movement of the vehicles causes a significant Doppler shift in the transmitted signals. This shift results in frequency variations that can lead to signal distortion and reduced SNR. Additionally, the faster-fading rates in high-speed scenarios introduce greater channel variability, causing fluctuations in signal strength over short periods. These effects collectively contribute to lower energy harvesting levels in high-speed scenarios than in low-speed scenarios despite similar configurations of RIS elements and UEs.

In conclusion, the energy harvested results are a culmination of various factors, including the synergistic effects of OFDM and RIS technologies, as well as the spatial distribution of UEs in a grid-like fashion with 50-meter spacing. This collective synergy highlights the potential of these technologies in enabling efficient energy harvesting in wireless communication systems.

2) ENERGY EFFICIENCY CALCULATION FOR FEEDBACK DNN 64QAM

In this subsection, we present the exact energy efficiency values for "Feedback DNN 64QAM" for 40 E0/N0 in a low-speed scenario for different numbers of transmissions. In our analysis, we assume a constant energy consumption per transmission throughout the study. Additionally, our data rates are derived from the provided Bit Error Rate (BER) values and represent achievable throughputs. Furthermore, we simplify our calculations by assuming that each transmission is error-free. Lastly, it's important to note that our energy efficiency calculations do not consider any additional system overhead or signaling energy consumption. We also examined by sending a 100 Mb (Megabit) file.

a: ENERGY EFFICIENCY COMPUTATION

The energy efficiency η in a given scenario is determined using the formula below:

$$\eta = \frac{\mathbf{T}}{\mathbf{E}}$$

where:

- $\mathbf{T}$ (Total Achievable Throughput): Calculated as the sum of data rates for each transmission, given by $\mathbf{T} = \sum_{i=1}^{\mathbf{N}} \mathbf{R_i}$, where $\mathbf{N}$ is the number of transmissions and $\mathbf{R_i}$ is the data rate for the i-th transmission.
- $\mathbf{E}$ (Energy Consumption): Estimated by the total energy used for $\mathbf{N}$ transmissions, represented as $\mathbf{E} = \mathbf{N} \cdot \mathbf{E}_{\text{per transmission}}$, where $\mathbf{E}_{\text{per transmission}}$ is the energy consumed per transmission.

Additional Parameters:

- $\mathbf{N}$ (Number of Transmissions): Varied to evaluate energy efficiency across different scenarios.
- $\mathbf{R_i}$ (Data Rate): Obtained from the Bit Error Rate (BER) values for "Feedback DNN 64QAM" at specific 40 E0/N0 values.
- $\mathbf{E}_{\text{per transmission}}$ (Energy Consumption per Transmission): Assumed to be constant per transmission, based on the given data and specific scenario.

b: RESULTS

Now, let's present the exact energy efficiency values for the "Feedback DNN 64QAM" for various numbers of transmissions.

TABLE 8. Energy efficiency calculation for feedback DNN 64QAM & 40 Eo/N0.

Number of Transmissions	Total Achievable Throughput (bits)	Energy Efficiency (bits/Joule)
100	0.0011 bits	0.0324 bits/Joule
200	0.0022 bits	0.0649 bits/Joule
300	0.0033 bits	0.0973 bits/Joule
400	0.0044 bits	0.1297 bits/Joule
500	0.0055 bits	0.1621 bits/Joule

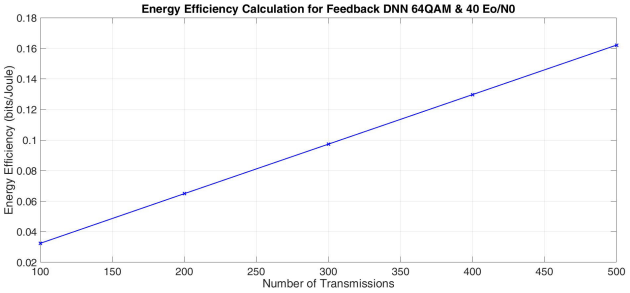

FIGURE 13. Energy efficiency calculation for feedback DNN 64QAM & 40 Eo/N0.

Examination: Sending a 100 Mb File via our system (100 Megabits = 12.5 Megabytes). Thus, 100 Megabits equals 2950.14 Megabits/Joule Energy Efficiency!

Table 8 presents the precise energy efficiency values for "Feedback DNN 64QAM" for various numbers of transmissions, along with the methodology, parameters explanation, and assumptions used in the calculations. The energy efficiency values indicate the number of bits that can be transmitted per Joule of energy consumed. The energy efficiency values represent the number of bits transmitted per Joule of energy consumed. As the number of transmissions increases, the energy efficiency improves, indicating higher data transmission capability per energy unit. The results in the table above show the total achievable throughput and energy efficiency for different numbers of transmissions. We also examined sending a 100 Mb file, where each transmission represents a symbol and the symbol represents 6 bits for 64QAM. The relationship between the number of transmissions and energy efficiency for a Feedback DNN 64QAM system under the condition of 40 Eo/N0 is presented in Figure 13. As the number of transmissions grows, a linear increase in energy efficiency is observed, suggesting that the system becomes more energy-efficient with an increased number of transmissions.

G. COMPARISON WITH OTHER ML APPROACHES

Figure 14 and Table 9 illustrates the cumulative energy efficiency of three distinct technical techniques about the number of transmissions. The methods employed include Feedback DNN 64QAM, indicated by a blue line with triangle markers; DPA TA 64QAM, represented as a black line with square markers; and LSTM [30], depicted by a red line with circle markers. Within the framework of 25 RIS

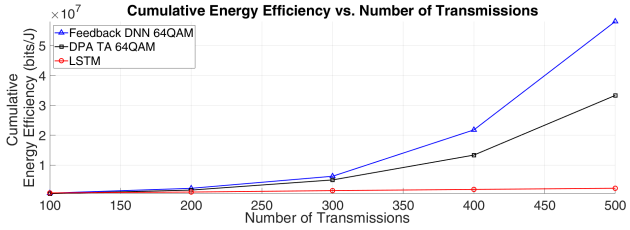

FIGURE 14. Cumulative Energy efficiency vs. Number of transmissions.

TABLE 9. Cumulative Energy efficiency vs. Number of transmissions.

Number of Transmissions	Feedback DNN 64QAM (bits/J)	DPA TA 64QAM (bits/J)	LSTM (bits/J)
100	0.58 million	0.40 million	0.65 million
200	2.19 million	1.60 million	0.94 million
300	6.23 million	5.00 million	1.42 million
400	21.78 million	13.33 million	1.82 million
500	58.12 million	33.33 million	2.21 million

elements and an SNR represented by 40 E0/N0, the energy efficiency of the Feedback DNN 64QAM exhibits a non-linear growth, with a distinct change in direction happening after 200 transmissions. This indicates a substantial increase in efficiency when the transmission numbers are higher. The efficiency of the DPA TA 64QAM increases linearly, consistently improving its performance without surpassing the Feedback DNN 64QAM at any given time. In contrast, the Proposed LSTM exhibits the least energy efficiency throughout the whole range, with a little and almost proportional improvement in efficiency as the number of transmissions increases. The graph demonstrates that the Feedback DNN 64QAM method exhibits significantly higher cumulative energy efficiency, especially after 200 transmissions. This suggests that it is well-suited for scenarios with high transmission rates and is crucial for energy-sensitive systems.

1) COMPARISON OF PERFORMANCE METRICS WITH LITERATURE REVIEW

The comprehensive evaluation provided in Table 10 elucidates the comparative strengths and limitations of various ML strategies applied to RIS for beam management. Our methodology, centered around the FeedbackDNN with 64QAM, emerges as a standout, delivering unparalleled performance across essential metrics including accuracy, energy efficiency, adaptability to high mobility scenarios, and the reduction of pilot overhead. This underscores our approach's efficacy in navigating the intricacies of RIS beamforming optimization within dynamic environments, as detailed in Table 10. In contrast, the endeavors by Wu and Zhang [16] and Huang et al. [17] underscore potential in aspects like network coverage enhancement and significant energy efficiency, albeit revealing gaps in adaptability to rapid environmental shifts and the degree of pilot overhead diminution. Subsequent works, such as those by Huang et al. [18] and Dai and Wei [22], yield

TABLE 10. Comparative analysis of performance metrics for ML-based RIS beam management techniques.

Reference	Accuracy (%)	Energy Efficiency	Pilot Overhead Reduction (%)	Adaptability to High Mobility
Our Approach	Superior	High	Significant	Excellent
Wu et al. [16]	Moderate	Improved	Moderate	Low
Huang et al. [17]	High	Very High	Low	Moderate
Huang et al. [18]	Moderate	High	Moderate	Low
Dai et al. [22]	High	Moderate	High	Moderate
Liu et al. [32]	High	Moderate	Very High	Low
Vu et al. [19]	Moderate	High	High	Moderate
Yang et al. [21]	High	Moderate	Moderate	High
Mahmood et al. [23]	Moderate	High	Low	Moderate
Huang et al. [24]	High	High	Moderate	Moderate
Zhong et al. [25]	Moderate	Moderate	High	Low
Elbir et al. [26]	High	Moderate	High	Moderate
Zou et al. [28]	Moderate	High	Moderate	Moderate
Gizzini et al. [29]	High	Moderate	Low	High
Gupta et al. [30]	High	Very High	Moderate	High
Ren et al. [31]	Moderate	High	Very High	Moderate

moderate to high ameliorations in MISO communication enhancement and downlink channel estimation, albeit grappling with challenges in high mobility adaptability and variable performance across different channel conditions. Efforts by Liu et al. [32] and Vu et al. [19], prioritizing pilot overhead reduction and the optimization of RIS configurations for dynamic channel conditions, achieve mixed results in terms of energy efficiency and adaptability. Similarly, contributions from Mahmood et al. [23], Huang et al. [24], and Zhong et al. [25], which address complex channel information needs, routing efficiency in multi-hop networks, and throughput optimization via RIS phase shift control, confront complications in computational complexity and the implementation within highly dynamic environments. Moreover, advancements by Elbir and Coleri [26], Zou et al. [28], Gizzini et al. [29], and Gupta et al. [30] in efficient channel prediction, throughput and resource use optimization among IoT devices, and the maximization of energy harvesting in wireless communications, while significant, acknowledge limitations tied to local dataset diversity, the dichotomy of immediate versus long-term throughput optimization, and the exigency for real-time context adaptation. The strategy delineated by Ren et al. [31], focused on curtailing channel estimation overhead through long-term CSI-based design, marks a commendable stride in net throughput efficiency, illustrating the multifarious tactics deployed by researchers to bolster RIS-augmented communication systems. Each study offers distinct contributions to the domain, with our approach marking a distinctive performance advantage, particularly in scenarios necessitating elevated adaptability and efficiency, as elaborated in Table 10.

H. OVERALL REMARKS

The in-depth analysis presented in the foregoing sections has provided a comprehensive overview of the performance of several advanced ML techniques in high and low-mobility scenarios. Specifically, the modulation approaches of LSTM, BLSTM, RNN_BLSTM, RNN, and FeedbackDNN have been critically assessed in their ability to predict the maximum signal achievable by training them with a generated dataset that is created using the 5G toolbox in Matlab and through brute force investigation of all phases of all the cases of signals as input (with constant m beams and n reflector elements) and selecting the maximum signal achieved with its characteristics by each case as output variable to be trained by our models. Thus, next, by keeping a specific data rate less than the achievable data rate, the element in RIS can utilize the excess power to charge. Thus we reduced the power consumption of the element by keeping the data rate constant and reducing transmission power. The whole scenario is shown in the BER (between BS and RIS) and, most specifically, in Figures 10 and 11.

From the evaluations, several conclusions can be drawn:

- LSTM models have proven their capability in predicting signals with satisfactory accuracy, particularly in capturing the overall trends of the data. However, they may occasionally exhibit minor delays in detecting rapid fluctuations, hinting at potential areas of improvement.
- The BLSTM model's bidirectional approach affords it a holistic understanding of the input data, allowing it to capture patterns that might otherwise be overlooked. Although the model demonstrated strong predictive capabilities, there is potential for further refinement, especially in its reaction to sudden shifts in data.
- RNNs, being adept at processing sequences, demonstrate strong predictive capabilities for time-varying scenarios. Despite this, a closer examination of their training dynamics underscores the significance of mitigating overfitting, especially in the later stages of the training process.
- FeedbackDNNs have emerged as a particularly robust model. Incorporating feedback mechanisms has rendered them adaptable, allowing them to recalibrate based on the output's accuracy. This ensures heightened robustness, especially in dynamic environments.
- The RNN_BLSTM model's fusion of traditional RNN with BLSTM offers enriched temporal dynamics, leading to improved learning capabilities. Its performance

highlights the benefits of combining the strengths of both RNNs and BLSTMs.

Furthermore, a joint comparison of all the approaches reveals that the FeedbackDNN model, in particular, stands out due to its consistently low loss values across various metrics, indicating superior predictive capabilities. This suggests that FeedbackDNN might be an optimal choice for beam management in RIS systems. However, it's imperative to consider the trade-offs between prediction accuracy and computational efficiency, particularly in real-world applications with stringent latency requirements.

Additionally, the analysis demonstrates that as the number of RIS elements increases, so does the energy harvesting capability of the system, suggesting that a larger number of RIS elements can significantly improve energy harvesting in Feedback DNN 64QAM communication systems. This is crucial in wireless communication scenarios with energy-constrained devices. Additionally, the energy efficiency calculations show a trend of increasing efficiency with the number of transmissions, highlighting the potential of the Feedback DNN 64QAM approach in energy-sensitive systems.

In conclusion, while each ML technique and RIS configuration has its strengths and areas of improvement, the continued evolution and refinement of these models and configurations remain paramount. The insights garnered from this analysis spotlight the current state-of-the-art and pave the way for future research. This research is expected to drive further advancements in the realm of high-mobility scenarios, RIS performance optimization, and energy-efficient communication systems.

VI. CONCLUSION AND FUTURE WORK

This study thoroughly investigates advanced ML techniques, specifically examining their suitability and efficacy in situations involving high mobility in RIS. The primary emphasis is placed on utilizing LSTM, BLSTM, RNN_BLSTM, RNN, and FeedbackDNN neural network architectures to predict the maximum attainable signal from BS and RIS by using specific modulation techniques (i.e., BPSK, QPSK, 64QAM). The results of our study suggest that LSTM models, although proficient in identifying general patterns in data, may need help to accurately capture sudden and quick changes. This observation underscores the possibility of significantly enhancing their response time. On the other hand, the bidirectional character of BLSTM models enables a more comprehensive comprehension of the incoming data. Although generally accurate, there are situations in which it responds slowly to sudden changes in data. RNNs, due to their intrinsic capacity to process sequential data, exhibited robust predictive capabilities in time-series contexts. However, upon further analysis of their training phase, it becomes evident that there is a significant emphasis on the importance of preventing overfitting, especially in the later stages. The Feedback DNN model emerged as the most prominent model in our investigation. Integrating feedback loops in the model improves its adaptability and allows for self-correction based on the accuracy of its outputs. The design decision enhances the system's durability, rendering it well-suited for dynamic situations. The hybrid model, known as RNN_BLSTM, demonstrated the potential of combining the strengths of both RNNs and BLSTMs, highlighting the effectiveness of synergistic techniques. Nevertheless, the performance of the subject, albeit impressive, highlighted certain aspects that may be enhanced. The Feedback DNN constantly showed superiority when evaluating all models because of its consistently low loss values across many measures. The model's predictive capabilities indicate that it could be the preferred choice for beam management in RIS systems. Nevertheless, it is crucial to consider the trade-off between the accuracy of predictions and the processing resources required, particularly in practical situations where minimizing latency is of utmost importance.

In summary, this study offers a comprehensive analysis of the capabilities and potential areas for improvement of several ML techniques in high and low-mobility scenarios using RIS. As ML progresses, our discoveries provide significant insights that can inform forthcoming investigations, aiming to enhance RIS performance by employing ongoing model enhancement. Moreover, our analysis has yielded two key findings relevant to the performance of Feedback DNN 64QAM communication systems. First, we observed that an increase in the number of Reconfigurable Intelligent Surface (RIS) elements leads to enhanced energy harvesting capabilities. This is a significant insight, especially for scenarios involving devices with constrained energy resources. Such an improvement in energy harvesting with more RIS elements could prove vital in optimizing the energy efficiency of wireless communication systems. Second, our energy efficiency calculations revealed a positive correlation between the number of transmissions and the system's energy efficiency. This trend highlights the potential of the Feedback DNN 64QAM approach in scenarios where energy efficiency is a critical consideration. These findings not only contribute to our understanding of the role of RIS in communication systems but also underscore the importance of optimizing transmission strategies for energy-sensitive applications.

For future work, we aim to extend the scope of our research by addressing the practical multi-user scenario with random positions of UEs, which presents a more complex and realistic challenge in wireless communication systems. While our current study has made significant strides in optimizing beam control in Reconfigurable Intelligent Surfaces (RISs) for a single user, we recognize the necessity of considering the dynamics and interactions of multiple users to fully leverage the potential of RIS technology beyond 5G systems. By focusing on multi-user environments, we plan to develop and refine our Feedback DNN strategy to accommodate the intricate balance required for efficient beamforming and steering among numerous users. This advancement will enhance our understanding of RIS capabilities in more

complex scenarios and contribute to the design of more robust and effective wireless communication systems capable of supporting high-density user environments.

APPENDIX A ADDITIONAL INFORMATION REGARDING IMPLEMENTATION AND FEATURES DESCRIPTION AND TERMS EXPLANAITION

This Appendix Section (Appendix Section A) provides the required information regarding communications terminology explanation for the user to understand the selection of features. The Appendix Section B indicates the provided code URL in GitHub and provides the code licensing directions.

A. TERMS EXPLANATION

- **HLS_Structure**[2]:
  - Represents a complex-valued matrix, with its real and imaginary parts utilized separately in the dataset.
  - Given the wireless communication context, ''HLS'' is related to *channel state information* or *signal representation*.
- **scheme_Channels_Structure**:
  - A complex-valued 3D array, of which real and imaginary parts (excluding the last column) are derived for dataset construction.
- **RHP** and **IHP**:
  - Represents the real and imaginary portions of the signal, **scheme_Channels_Structure**, excluding its last column.
- **True_Channels_Structure**:
  - A complex-valued structure from which both real and imaginary parts are processed individually.
  - The extracted values based on specific indices (‘dpositions‘) represent the actual or ground-truth channel values or features. The dpossitions represent the positions of the data subcarriers within the set of all active subcarriers (denoted by Kset in the code) that the Channel uses.

[2]The ''Hybrid Learning Structure'' (HLS), as introduced in our manuscript and associated with Algorithm-1, plays a pivotal role in enhancing the efficiency and effectiveness of RIS-aided communication systems. This framework is designed to amalgamate multiple sources of Channel State Information (CSI), thereby optimizing signal processing within RIS systems. By leveraging the integration of both direct and reflective path information, the HLS significantly improves the accuracy of signal prediction and overall system performance. This comprehensive approach is detailed in Appendix-A, where we delve into the operational intricacies of the HLS and its critical function in advancing RIS technology for superior communication networks. Particularly in scenarios lacking a direct line of sight, the HLS facilitates a dynamic adaptation of the RIS, promoting seamless and energy-efficient communication. Through this framework, as illustrated in Sections IV-B2, 1, and 2, our research underscores the transformative potential of combining ML with telecommunication technologies to refine and exploit the capabilities of RIS, thereby setting a new benchmark for optimized communication in high-mobility scenarios.

B. FEATURES OF DATASET_X & DATASET_Y

1) **True_Channels_Structure(:,:,n_ch) = hfC(Kset,:);** label=-
   - `True_Channels_Structure`: This variable is a 3D structure that stores information about multiple channels or paths. It contains the actual channel characteristics.
   - `n_ch`: Typically represents an index referring to the ''n-th channel.'' This allows the user to address and store data for multiple channels.
   - `hfC`: Given the context, this represents the channel frequency response or coefficients. The ‘h’ denotes a channel in signal processing, and ‘fC’ could imply frequency coefficients.
   - `Kset`: This is a set or list of indices (ppositions/dpositions). The specific rows from the `hfC` matrix corresponding to these indices (ppositions/dpositions) are being fetched.
2) **HLS_Structure(:,n_ch) = he_LS_Preamble;** label=-
   - `HLS_Structure`: A 2D structure stores information related to some form of preamble for multiple channels. ‘HLS’ denotes a specific type of preamble or sequence used in the system.
   - `he_LS_Preamble`: This is a Long Sequence (LS) preamble. Preambles are known sequences sent at the beginning of a transmission to help the receiver with synchronization, channel estimation, etc. The ‘he’ prefix shows that this preamble is for High-Efficiency (HE) mode (IEEE 802.11p LS Estimate at Preambles).
3) **DPA_TA_Structure(:,:,n_ch) = H_DPA_TA;** label=-
   - `DPA_TA_Structure`: A 3D structure, similar in form to `True_Channels_Structure`. It stores Time Alignment (‘TA‘) information for multiple channels. ‘DPA’ might denote a specific technique or protocol in use.
   - `H_DPA_TA`: represents the DPA technique's actual Time Alignment data or coefficients. Time Alignment typically refers to adjusting the timing of signals, especially in multi-path or multi-antenna scenarios, to ensure proper synchronization.

C. A SYMBOLIC REPRESENTATION OF THE RIS-BASED SIGNAL PROCESSING APPROACH

This section provides a more symbolic representation of our approach in the following algorithm (Algorithm 4).

APPENDIX B CODE REPOSITORY

The source code to implement the work reported in this paper is available in the GitHub repository at the following URL: https://github.com/NETRL/DeepRISBeam.git

Algorithm 4 RIS-Based Signal Processing Approach

procedure $\mathcal{RIS}$
  Initialization:
  $N_{samples} \leftarrow 1000$
  $N_{train} \leftarrow 0.8 \times N_{samples}$, $N_{test} \leftarrow 0.2 \times N_{samples}$
  $I_{train} \leftarrow \text{Random}(N_{train})$, $I_{test} \leftarrow N_{samples} \setminus I_{train}$
  Save I_{train}, I_{test} to '.mat'
  Generate Datasets:
  Define $\Theta_{OFDM}, \Theta_{mod}, \Theta_{scram}, \Theta_{code}, \Theta_{intl}, \Theta_{chan}, \Theta_{sim}$
  for each $EbN0dB$ **do**
    Simulate $\leftrightarrow$ Transmit/Receive
    $H_{est} \leftarrow$ LS Estimate
    Decode, Store Metrics
  end for
  Save $\Theta_{config}, BER, NMSE$
  Prepare ML Datasets:
  Load I_{train}, I_{test}
  for config $\in \{train, test\}$ **do**
    Set $\Theta_{loop}, \Theta_{sim}$
    for each $EbN0dB$ **do**
      Load Results
      Input $\mathcal{X}$**:**
      $\mathcal{X} \leftarrow$ Extract/Append $\mathcal{R}$(HLS), $\mathcal{I}$(HLS)
      Permute $\mathcal{X}$
      Output $\mathcal{Y}$**:**
      $\mathcal{Y} \leftarrow$ Extract/Append $\mathcal{R}$(True Channels), $\mathcal{I}$(True Channels)
      Permute $\mathcal{Y}$
      Save $\mathcal{X}, \mathcal{Y}$
    end for
  end for
end procedure

You can access and download the code and any necessary instructions or documentation from this repository. Feel free to refer to this repository for a detailed view of the codebase and its usage.

Note: Please ensure to comply with any licensing or usage terms specified in the repository.

REFERENCES

[1] C. Huang, C. Yuen, and H. Ren, Eds., *Reconfigurable Intelligent Surface-Empowered 6G. Wireless Networks*, 1st ed. Cham, Switzerland: Springer, 2021.

[2] L. Yang, P. Li, Y. Yang, S. Li, I. Trigui, and R. Ma, "Performance analysis of RIS-aided networks with co-channel interference," *IEEE Commun. Lett.*, vol. 26, no. 1, pp. 49–53, Jan. 2022.

[3] N. Ashraf, T. Saeed, H. Taghvaee, S. Abadal, V. Vassiliou, C. Liaskos, A. Pitsillides, and M. Lestas, "Intelligent beam steering for wireless communication using programmable metasurfaces," *IEEE Trans. Intell. Transp. Syst.*, vol. 24, no. 5, pp. 4848–4861, 2023.

[4] M. Xu, S. Zhang, C. Zhong, J. Ma, and O. A. Dobre, "Ordinary differential equation-based CNN for channel extrapolation over RIS-assisted communication," *IEEE Commun. Lett.*, vol. 25, no. 6, pp. 1921–1925, Jun. 2021.

[5] X. Jin, Y. Wang, H. Zhang, H. Zhong, L. Liu, Q. M. J. Wu, and Y. Yang, "DM-RIS: Deep multimodel rail inspection system with improved MRF-GMM and CNN," *IEEE Trans. Instrum. Meas.*, vol. 69, no. 4, pp. 1051–1065, Apr. 2020.

[6] Z. He, F. Héliot, and Y. Ma, "CNN-enabled joint active and passive beamforming for RIS-assisted MU-MIMO systems," in *Proc. IEEE 97th Veh. Technol. Conf. (VTC-Spring)*, Jun. 2023, pp. 1–6.

[7] M. Di Renzo, A. Zappone, M. Debbah, M.-S. Alouini, C. Yuen, J. de Rosny, and S. Tretyakov, "Smart radio environments empowered by reconfigurable intelligent surfaces: How it works, state of research, and the road ahead," *IEEE J. Sel. Areas Commun.*, vol. 38, no. 11, pp. 2450–2525, Nov. 2020.

[8] J. P. Lemayian and J. M. Hamamreh, "Recurrent neural network-based channel prediction in mMIMO for enhanced performance in future wireless communication," in *Proc. Int. Conf. U.K.-China Emerg. Technol. (UCET)*, China, Aug. 2020, pp. 1–4.

[9] M. S. Islam, R. Abozariba, A. T. Asyhari, M. Patwary, and M. A. Matin, "Feasibility of LDM to serve user-IoT pairs in the future wireless network," in *A Glimpse Beyond 5G in Wireless Networks*. Cham, Switzerland: Springer, 2022, pp. 231–253.

[10] S. Hochreiter and J. Schmidhuber, "Long short-term memory," *Neural Comput.*, vol. 9, no. 8, pp. 1735–1780, Nov. 1997.

[11] A. Graves and J. Schmidhuber, "Framewise phoneme classification with bidirectional LSTM and other neural network architectures," *Neural Netw.*, vol. 18, nos. 5–6, pp. 602–610, Jul. 2005.

[12] J. Elman, "Finding structure in time," *Cognit. Sci.*, vol. 14, no. 2, pp. 179–211, Jun. 1990.

[13] W. Bao, J. Yue, and Y. Rao, "A deep learning framework for financial time series using stacked autoencoders and long-short term memory," *PLoS ONE*, vol. 12, no. 7, Jul. 2017, Art. no. e0180944.

[14] A. Nøkland, "Direct feedback alignment provides learning in deep neural networks," in *Proc. Adv. Neural Inf. Process. Syst.*, vol. 29, 2016, pp. 1037–1045.

[15] S. Yan, X. Fang, B. Xiao, H. Rockwell, Y. Zhang, and T. S. Lee, "Recurrent feedback improves feedforward representations in deep neural networks," 2019, *arXiv:1912.10489*.

[16] Q. Wu and R. Zhang, "Intelligent reflecting surface enhanced wireless network via joint active and passive beamforming," *IEEE Trans. Wireless Commun.*, vol. 18, no. 11, pp. 5394–5409, Nov. 2019.

[17] C. Huang, A. Zappone, G. C. Alexandropoulos, M. Debbah, and C. Yuen, "Reconfigurable intelligent surfaces for energy efficiency in wireless communication," *IEEE Trans. Wireless Commun.*, vol. 18, no. 8, pp. 4157–4170, Aug. 2019.

[18] C. Huang, R. Mo, and C. Yuen, "Reconfigurable intelligent surface assisted multiuser MISO systems exploiting deep reinforcement learning," *IEEE J. Sel. Areas Commun.*, vol. 38, no. 8, pp. 1839–1850, Aug. 2020.

[19] T.-H. Vu, T.-V. Nguyen, D. B. da Costa, and S. Kim, "Reconfigurable intelligent surface-aided cognitive NOMA networks: Performance analysis and deep learning evaluation," *IEEE Trans. Wireless Commun.*, vol. 21, no. 12, pp. 10662–10677, Dec. 2022.

[20] K.-T. Nguyen, T.-H. Vu, and S. Kim, "Performance analysis and deep learning design of short-packet communication in multi-RIS-aided multiantenna wireless systems," *IEEE Internet Things J.*, vol. 10, no. 19, pp. 17265–17281, Oct. 2023.

[21] Z. Yang, Y. Liu, Y. Chen, and N. Al-Dhahir, "Machine learning for user partitioning and phase shifters design in RIS-aided NOMA networks," *IEEE Trans. Commun.*, vol. 69, no. 11, pp. 7414–7428, Nov. 2021.

[22] L. Dai and X. Wei, "Distributed machine learning based downlink channel estimation for RIS assisted wireless communications," *IEEE Trans. Commun.*, vol. 70, no. 7, pp. 4900–4909, Jul. 2022.

[23] M. R. Mahmood, M. A. Matin, and S. K. Goudos, "RIS-assisted multi-user MIMO systems exploiting extreme learning machine," *IEEE Access*, vol. 11, pp. 47129–47136, 2023.

[24] C. Huang, G. Chen, J. Tang, P. Xiao, and Z. Han, "Machine-learning-empowered passive beamforming and routing design for multi-RIS-assisted multihop networks," *IEEE Internet Things J.*, vol. 9, no. 24, pp. 25673–25684, Dec. 2022.

[25] R. Zhong, Y. Liu, X. Mu, Y. Chen, and L. Song, "AI empowered RIS-assisted NOMA networks: Deep learning or reinforcement learning?" *IEEE J. Sel. Areas Commun.*, vol. 40, no. 1, pp. 182–196, Jan. 2022.

[26] A. M. Elbir and S. Coleri, "Federated learning for channel estimation in conventional and RIS-assisted massive MIMO," *IEEE Trans. Wireless Commun.*, vol. 21, no. 6, pp. 4255–4268, Jun. 2022.

[27] H. Liu, X. Yuan, and Y. A. Zhang, "Joint communication-learning design for RIS-assisted federated learning," in *Proc. IEEE Int. Conf. Commun. Workshops (ICC Workshops)*, Jun. 2021, pp. 1–6.
[28] Y. Zou, Y. Liu, X. Mu, X. Zhang, Y. Liu, and C. Yuen, "Machine learning in RIS-assisted NOMA IoT networks," *IEEE Internet Things J.*, vol. 10, no. 22, pp. 19427–19440, 2023, doi: 10.1109/JIOT.2023.3245288.
[29] A. K. Gizzini, M. Chafii, S. Ehsanfar, and R. M. Shubair, "Temporal averaging LSTM-based channel estimation scheme for IEEE 802.11p standard," in *Proc. IEEE Global Commun. Conf. (GLOBECOM)*, Dec. 2021, pp. 1–7.
[30] K. D. Gupta, R. Nigam, D. K. Sharma, and S. K. Dhurandher, "LSTM-based energy-efficient wireless communication with reconfigurable intelligent surfaces," *IEEE Trans. Green Commun. Netw.*, vol. 6, no. 2, pp. 704–712, Jun. 2022.
[31] H. Ren, C. Pan, L. Wang, W. Liu, Z. Kou, and K. Wang, "Long-term CSI-based design for RIS-aided multiuser MISO systems exploiting deep reinforcement learning," *IEEE Commun. Lett.*, vol. 26, no. 3, pp. 567–571, Mar. 2022.
[32] W. Liu, C. Pan, H. Ren, F. Shu, S. Jin, and J. Wang, "Low-overhead beam training scheme for extremely large-scale RIS in near field," *IEEE Trans. Commun.*, vol. 71, no. 8, pp. 4924–4940, 2023, doi: 10.1109/TCOMM.2023.3278728.
[33] C. Pan, G. Zhou, K. Zhi, S. Hong, T. Wu, Y. Pan, H. Ren, M. D. Renzo, A. Lee Swindlehurst, R. Zhang, and A. Y. Zhang, "An overview of signal processing techniques for RIS/IRS-aided wireless systems," *IEEE J. Sel. Topics Signal Process.*, vol. 16, no. 5, pp. 883–917, Aug. 2022.
[34] C. Pan, R. Zhang, M. Di Renzo, A. L. Swindlehurst, and Y. A. Zhang, "Editorial introduction to the issue on advanced signal processing for reconfigurable intelligent surface-aided 6G networks," *IEEE J. Sel. Topics Signal Process.*, vol. 16, no. 5, pp. 880–882, Aug. 2022.
[35] M. Rossanese, P. Mursia, A. Garcia-Saavedra, V. Sciancalepore, A. Asadi, and X. Costa-Pérez, "RIS-power-measurements-dataset," *IEEE Dataport*, 2022, doi: 10.21227/tj39-zr48.
[36] S. Tewes, M. Heinrichs, K. Weinberger, R. Kronberger, and A. Sezgin, "A comprehensive dataset of RIS-based channel measurements in the 5GHz band," in *Proc. IEEE 97th Veh. Technol. Conf. (VTC-Spring)*, Jun. 2023, pp. 2814–2815.
[37] J. Peng and G. J. Snyder, "A figure of merit for flexibility," *Science*, vol. 366, no. 6466, pp. 690–691, Nov. 2019.
[38] W. Koehrsen, "Overfitting vs. underfitting: A complete example," in *Towards Data Science*, vol. 405, 2018. [Online]. Available: https://towardsdatascience.com/overfitting-vs-underfitting-a-complete-example-d3f6cacff677

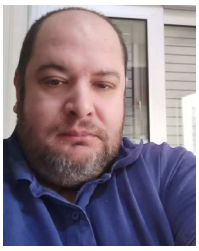

IACOVOS I. IOANNOU (Member, IEEE) received the Associate degree in computer science from Cyprus College, in 2001, the B.Sc. degree in computer science from the University of Cyprus, in 2006, the M.Sc. degree (Hons.) in computer and network security from the Open University of Cyprus, in 2017, and the Ph.D. degree from the University of Cyprus, in 2021, with a focus on telecommunications with AI/ML. He is a highly skilled developer with 20 years of hands-on working experience in the IT industry, ranging in the spectrum of IT systems from analysis, development, installation, and management. He was an IT Administrator and Programmer with the Philelefthetos Publishing Group for seven years. He was an IT and Programmer with the Cyprus Stock Exchange for seven years. He was an IT and Software Engineer with the Services Department, Primetel, for six years. He is currently a Researcher with the Networks Research Laboratory, University of Cyprus. He is also a Junior Researcher with the Smart Networked Systems Research Group, RISE Center. He has vast experience with cellular network infrastructure and all modern development platforms and languages. His research interests include mobile and wireless communications, next-generation networks (5G), and device-to-device (D2D) communications, using artificial intelligence techniques. He has a certificate in ICONIX/SCRUM. He is also CCNET Certified from CISCO.

MARIOS RASPOPOULOS (Member, IEEE) received the M.Sc. and M.Eng. degrees and the Ph.D. degree in telecommunications from the University of Surrey, in 2008.

His career has been marked by significant roles, including an Associate Professor with UCLan Cyprus, since 2021, and prior positions as an Assistant Professor with UCLan Cyprus, an Adjunct Lecturer with the Open University of Cyprus, the Chief Technical Officer with Sigint Solutions Ltd., and a Research Associate with the University of Surrey. He is an esteemed academic in the field of telecommunications. He is currently the Deputy Head of the School of Sciences and an Associate Professor. In his administrative capacity, he has led several committees and contributed significantly to the fields of innovation and enterprise in academia. His research interests include telecommunications, including 5G communications and electronic positioning. A member of several professional bodies, such as FHEA and ETEK, he also contributes to the IPIN International Standards Committee.

PRABAGARANE NAGARADJANE received the M.Tech. and Ph.D. degrees in ECE from Pondicherry Engineering College, Pondicherry (Central) University. He is currently an Associate Professor with the Department of Electronics and Communication Engineering, SSN Institutions. Before this, he was with HCL Info Systems for a brief period of two years. Recently, he visited the Beyond 5G Wireless Innovation Center, King Mongkut's University of Technology, North Bangkok, as a Short-Term Visitor. He has authored or coauthored more than 75 technical articles and two books. Furthermore, he has also coauthored a research book titled *Distributed Artificial Intelligence for 5G/6G Communications* (Taylor and Francis) and a textbook on *Electronic Communications* for AICTE e-KUMBH. His research interests include various aspects of wireless communications, especially concerning signal processing for wireless and broadband communications and the application of machine learning and artificial intelligence for wireless communications. He is one of the founding members of the Wireless Communications, Signal Processing and Networking (WiSPNET) International Conference technically co-sponsored by IEEE. He also served as one of the organizing chairs of 2016, 2017, 2018, 2020, 2021, and 2022 WiSPNET and the Co-Chair of the WiSPNET 2019 Conference. He is serving as the Organizing Chair of the IEEE technically co-sponsored AsianComNet 2024 Conference to be held in Thailand. He has guest-edited two special issues on the topic of signal processing for 5G in the *Computers and Electrical Engineering* journal (Elsevier). He also served on the editorial board of the *Physical Communication* journal as an Area Editor. He is currently an Associate Editor of *IET Communications* journal.

CHRISTOPHOROS CHRISTOPHOROU received the B.Sc. degree in computer science, the M.Sc. degree in advanced computer technologies, and the Ph.D. degree in mobile/wireless networks from the University of Cyprus, in 2002, 2005, and 2011, respectively.

Since 2004, he has been a Researcher and a Project Manager in different local (RPF-funded) and EU-funded research projects in the domain of AAL and ageing well, such as FRAIL, SUCCESS, MEMENTO, GrowMeUp, Miraculous-Life, SocialRobot, Co-Living, and AgeingWell; and in the mobile and wireless networks domain, such as C-CAST, C-MOBILE, MOTIVE, and BBONE. He has published over 35 papers in journals, scientific conferences, and book chapters. His research interests include the telecommunications and networking, database management systems, social collaborative care networks, and information and communication technology (ICT) personalized solutions (for various sectors, including the eHealth domain).

WAQAR ALI AZIZ received the B.Eng. degree in electrical engineering from the University of Engineering and Technology, Peshawar, Pakistan, in 2016, and the M.S. degree in electrical engineering from the National University of Sciences and Technology, Pakistan, in 2020. He is currently pursuing the Ph.D. degree with the Department of Computer Science, University of Cyprus. His research interests include the application of optimization methods in wireless networks, the use of metasurfaces in the next generation mobile networks, and deep learning in computer networks.

VASOS VASSILIOU (Senior Member, IEEE) has been the Group Leader with the Smart Networked Systems Research Group, CYENS Centre of Excellence, Nicosia, Cyprus, since November 2017. He is currently an Associate Professor with the Computer Science Department, University of Cyprus, and the Director of the Networks Research Laboratory (NetRL), UCY. His research interests include protocol design and performance aspects of networks (fixed, mobile, and wireless), in particular mobility management, QoS adaptation and control, resource allocation techniques, wireless sensor networks, and the Internet of Things. He is a Senior Member of ACM. He is on the editorial boards of the *Telecommunication Systems* journal (Springer) and *Computer Networks* journal (Elsevier).

ANDREAS PITSILLIDES is currently a Professor with the Department of Computer Science, University of Cyprus, and the Co-Director of the Networks Research Laboratory (NetRL, http://www.NetRL.cs.ucy.ac.cy). Before that, he was a Visiting Professor with the Department of Electrical and Electronic Engineering Science, University of Johannesburg, from 2021 to 2024. He was a Visiting Professor with the School of Electrical and Information Engineering, University of the Witwatersrand (Wits), from 2017 to 2020, and the Department of Electrical and Electronic Engineering Science, University of Johannesburg, South Africa, from 2014 to 2017. He has published over 350 refereed articles in flagship journals (e.g., IEEE, Elsevier, IFAC, and Springer), international conferences, and book chapters, coauthored two books (one edited), participated as the Principal or the Co-Principal Investigator in over 40 European Commission and locally funded research projects with over 6.7 million Euro. His research interests include communication networks, software-defined metamaterials (hypersurfaces and reconfigurable intelligent surfaces), nanonetworks and the Internet- and Web-of Things, smart systems (e.g., smart grid), smart spaces (e.g., home and city), and e-health. He has a particular interest in adapting tools from various fields of applied mathematics, such as adaptive non-linear control theory, computational intelligence, game theory, and complex systems and nature-inspired techniques, to solve problems in communication networks.

He received several awards, including the best paper, presented keynotes, invited lectures at major research organizations, short courses at international conferences, and short courses to industry.